Dust Polarization Results from Planck

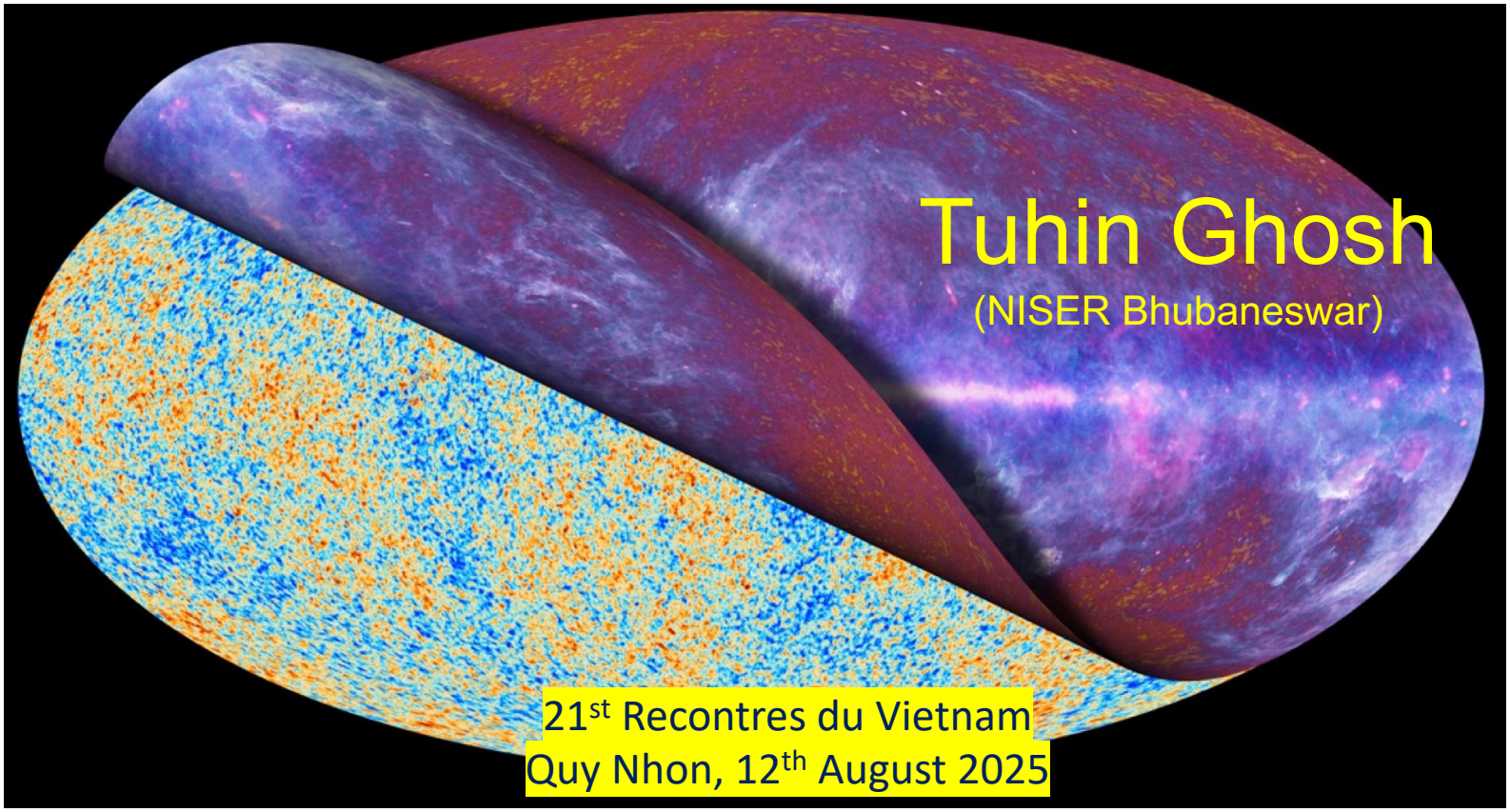

CMB experiments

Space-based

COBE-DMR (NASA)
1st generation
CMB experiment

31-90 GHz

WMAP (NASA)
2nd generation
CMB experiment

23-94 GHz

Planck (ESA
3rd generation
CMB experiment

30-857 GHz

Future

LiteBIRD (JAXA)

Matsumura et al, 2013

40 – 402 GHz

2.5 μK.arcmin

CMB BHARAT: AN INDIAN COSMOLOGY CONSORTIUM

CMB-Bharat

Ground-based

Simon's Observatory

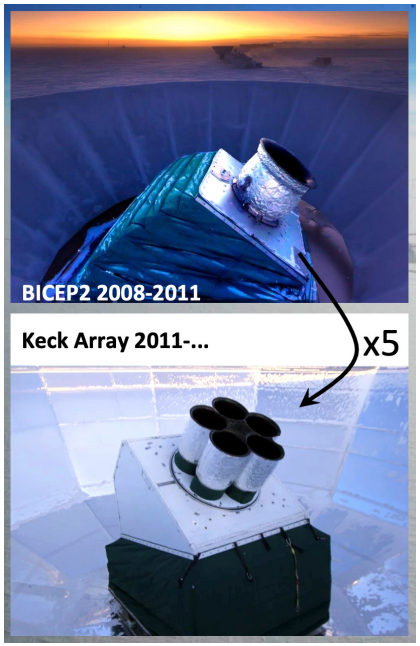

Foreground challenge

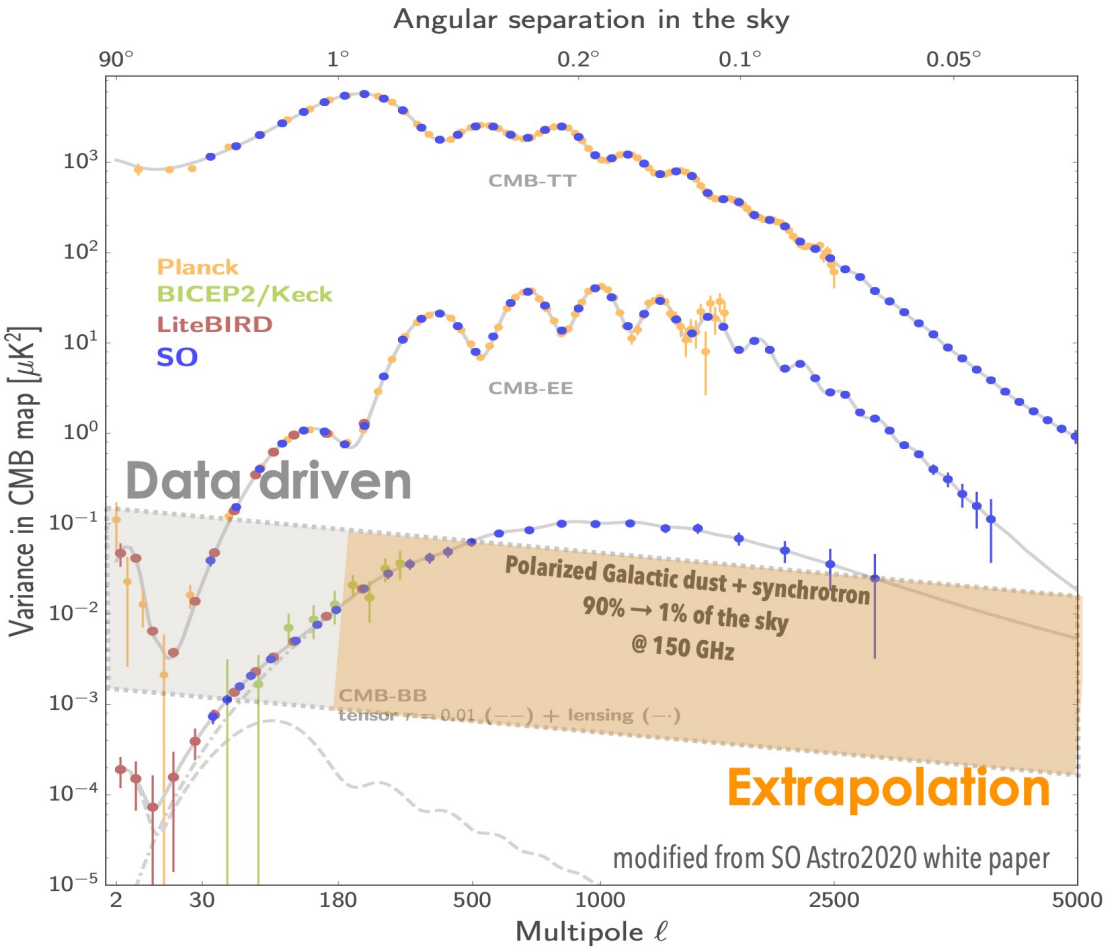

- From the available data (Planck + BICEP/Keck), we have information of large-scale polarized foregrounds.
- Statistical properties of foregrounds at small-scales are unknown.
- Foregrounds like CO emission may be relevant at small-scales.

SO Astro2020 white paper

Synchrotron Polarization

- Produce by relativistic cosmic ray electrons accelerating in the Galactic magnetic field (few uG)
- Dominates up to 80 GHz
- Upto 70% polarised (theoretically)
  ~40-50% max observed
  ~20% typical
- Follows power-law spectrum

$$Q_\nu = Q_{\nu_0}(\nu/\nu_0)^{\beta_s}$$
$$U_\nu = U_{\nu_0}(\nu/\nu_0)^{\beta_s}$$

- Steep spectrum β_s ~ -3.13 +/- 0.13
- Low frequencies (< few GHz) corrupted by Faraday Rotation

Synchrotron Polarized Intensity map

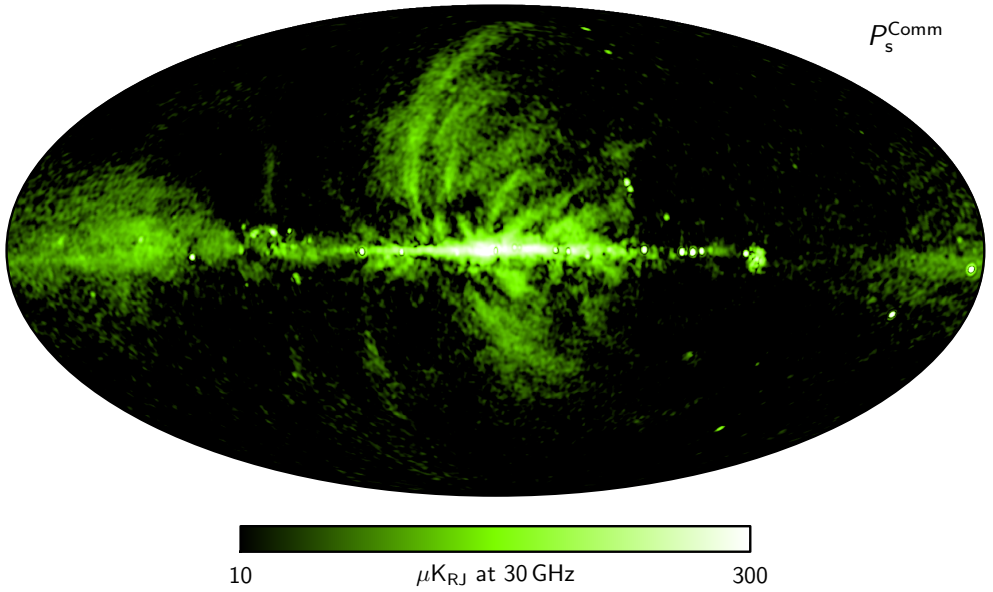

Planck 2018 results IV

Dust polarization

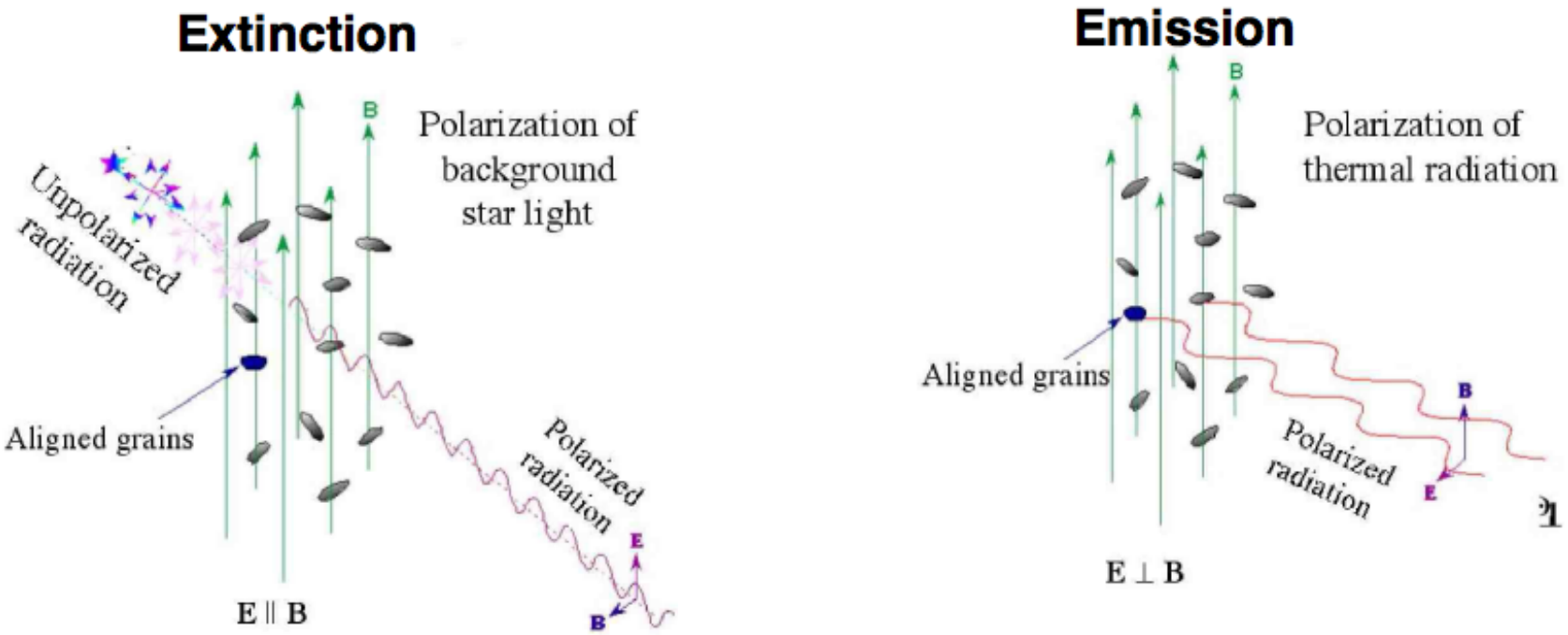

Lazarian 2008

- Unpolarized starlight absorbed by prolate rotating dust grains aligned with respect to the Galactic magnetic field and thermally emitted in the far infrared and millimeter frequencies.
- Polarized *perpendicular* to the magnetic field lines, up to ~20%
- Follows modified blackbody spectrum

$$Q_\nu = Q_{\nu_0}(\nu/\nu_0)^{\beta_d} B_\nu(T_d)$$

$$U_\nu = U_{\nu_0}(\nu/\nu_0)^{\beta_d} B_\nu(T_d)$$

- Dominant polarized emission at $\nu \gtrsim 70$ GHz

Challenge: Galactic and extra-Galactic foregrounds

Stokes *I* : Intensity

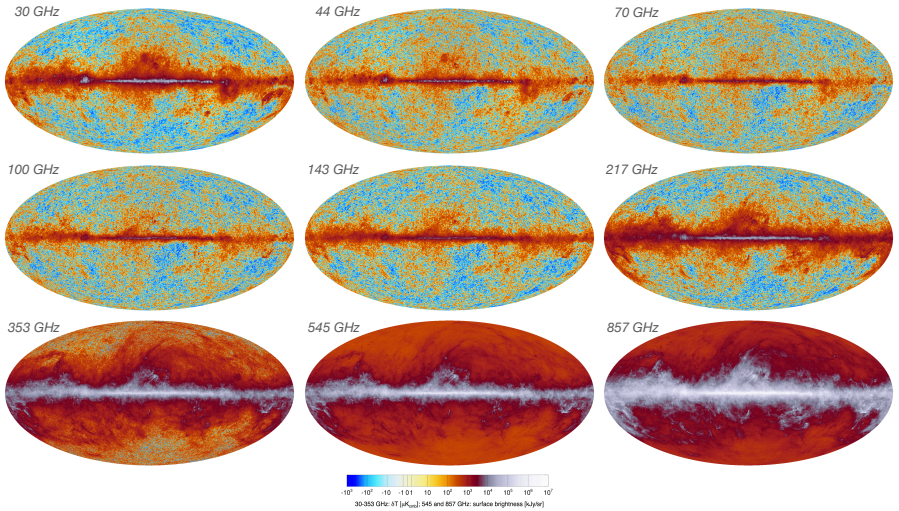

Polarization →

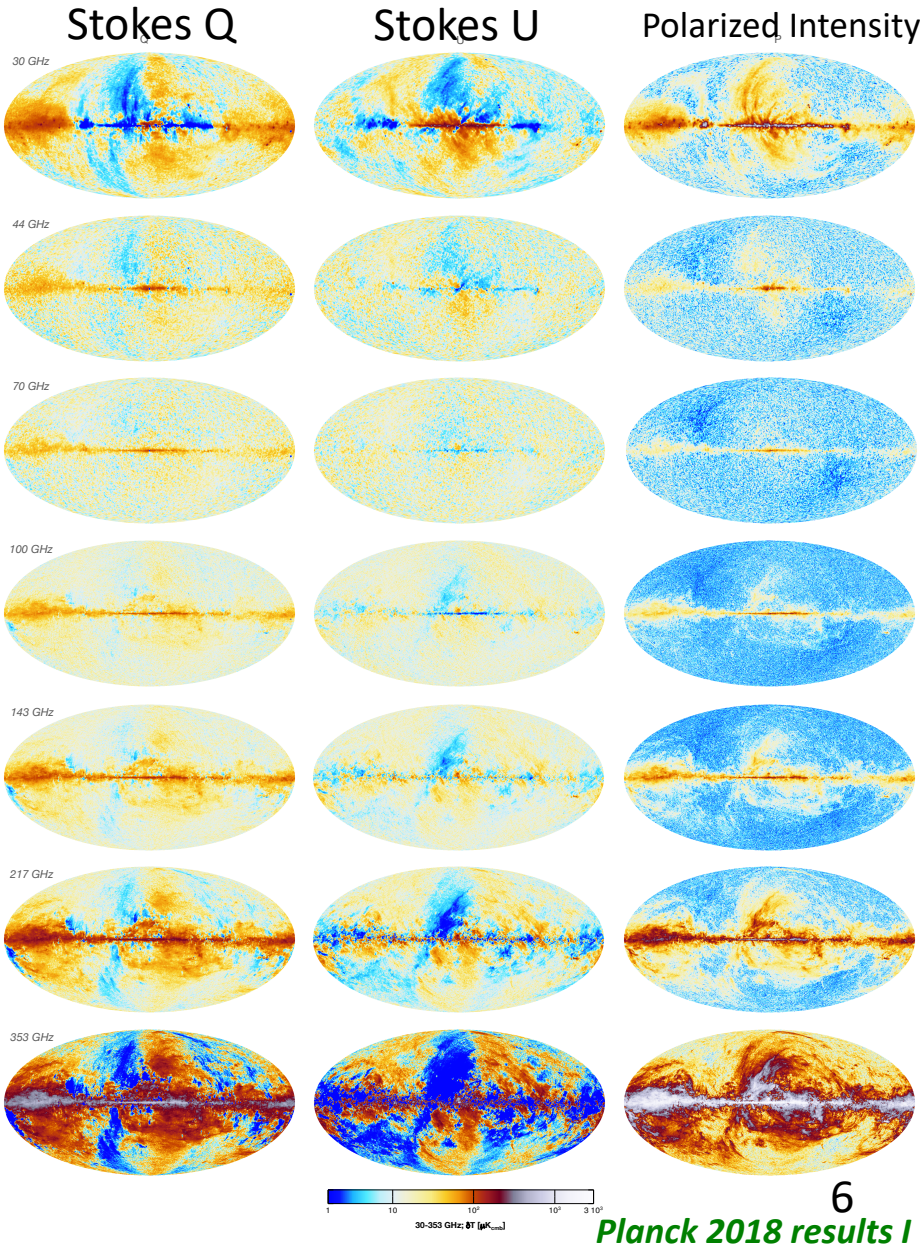

Stokes Parameters

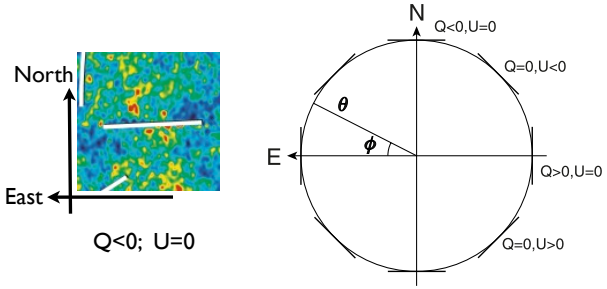

Planck 2018 results I

Foregrounds Spectral Energy Distribution (SED)

Recombination B-modes ℓ range

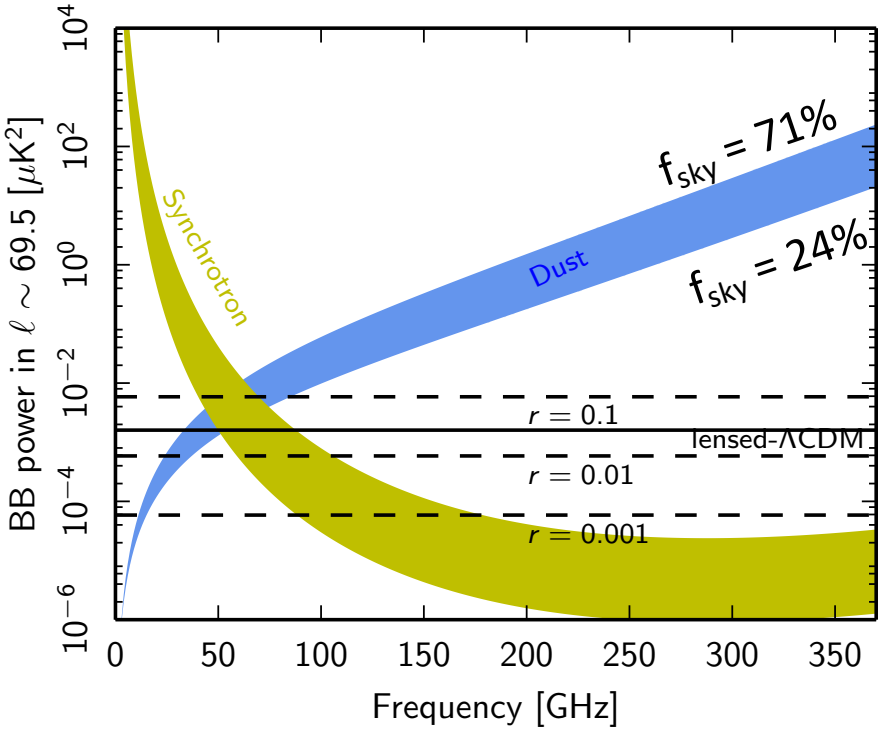

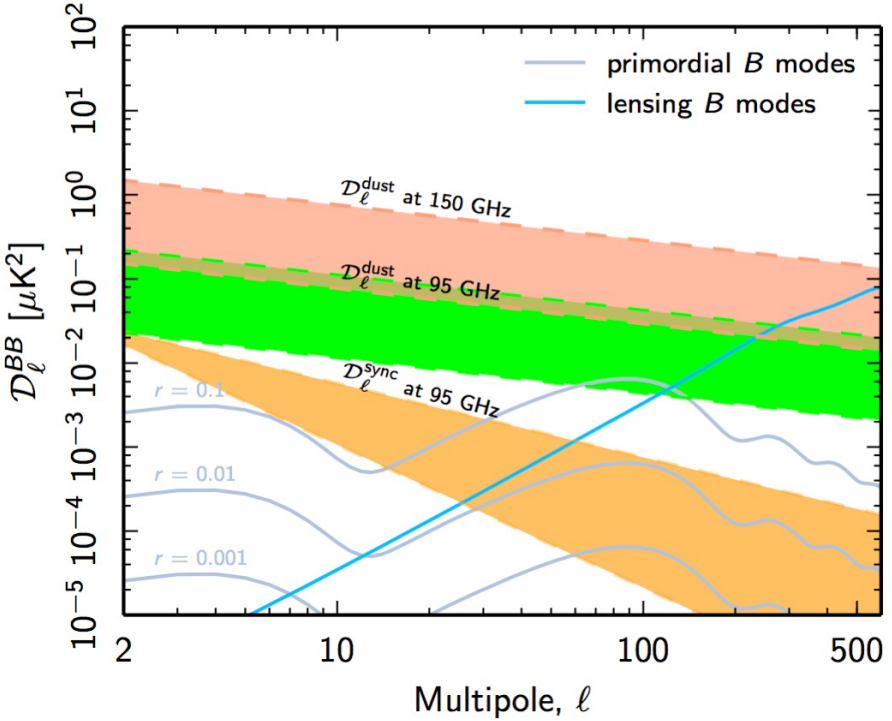

Planck 2018 results XI

- The frequency at which dust and synchrotron *B*-modes power are equal depends on multipole and sky region.
- Dust quickly dominates synchrotron at higher frequencies.

Model-dependent approach to extract CMB B-modes

Mismatch between model and the actual data

MODEL

$$m_\nu(\hat{n}) = a_\nu s_{\rm CMB}(\hat{n}) + \nu^{\beta_s} s_{\rm sync}(\hat{n}) + \nu^{\beta_d} B_\nu(T_d) s_{\rm dust}(\hat{n}) + n_\nu(\hat{n})$$

Inaccurate modeling of dust

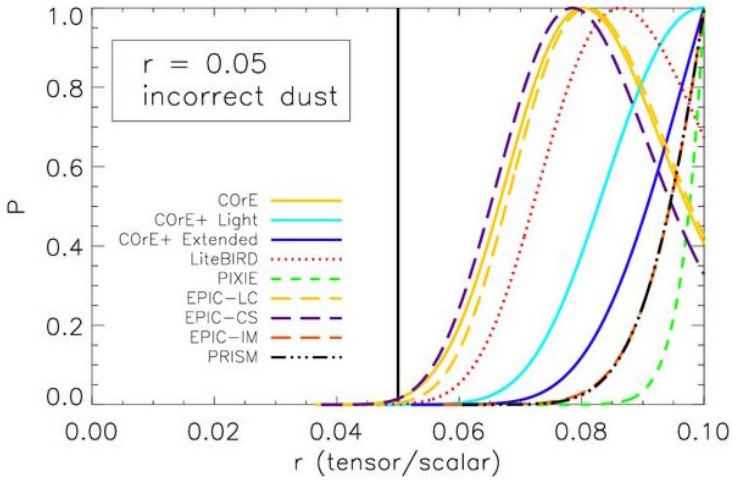

Remazeilles et al. 2016

Data:

1. Two-component dust model
2. Synchrotron curvature
3. Anomalous Microwave Emission (AME) polarization

- Three frequencies : 60 GHz (synchrotron channel), 100 GHz (CMB channel), 240 GHz (dust channel).
- 0.5 degree beam resolution
- 2 uK arcmnin noise sensitivity
- Target *r* sensitivity r ~ 10^{-3}

Katayama and Komatsu 2011

Dust amplitude at the map level:

$$d_\nu = A\,\nu^{\beta_d}\,B_\nu(T_d)$$

Dust amplitude at the power-spectrum level:

$$C_\ell^{d_{\nu_1}\times d_{\nu_2}} = K_\ell\,(\nu_1\nu_2)^{\beta_d}\,B_{\nu_1}(T_d)\,B_{\nu_2}(T_d)$$

$$= K_0\ell^{\alpha_d}\,(\nu_1\nu_2)^{\beta_d}\,B_{\nu_1}(T_d)\,B_{\nu_2}(T_d)$$

Multicomponent likelihood analysis

To fit all the measured spectra simultaneously with a model for BB that is primordial CMB B mode signal (*r*) + LCDM lensing expectation + 7 parameters foreground model

Amplitude of cross-spectra between frequencies ν_1 and ν_2 :

$$\mathcal{D}_\ell(\nu_1 \times \nu_2) = A_{\rm s}\left(\frac{\nu_1\nu_2}{28.4^2}\right)^{\beta_{\rm s}} + A_{\rm d}\left(\frac{\nu_1\nu_2}{353^2}\right)^{\beta_{\rm d}-2}\frac{B_{\nu_1}(T_{\rm d})}{B_{353}(T_{\rm d})}\frac{B_{\nu_2}(T_{\rm d})}{B_{353}(T_{\rm d})}$$
$$+ \rho\sqrt{A_{\rm s}A_{\rm d}}\left[\left(\frac{\nu_1}{28.4}\right)^{\beta_{\rm s}}\left(\frac{\nu_2}{353}\right)^{\beta_{\rm d}-2}\frac{B_{\nu_2}(T_{\rm d})}{B_{353}(T_{\rm d})}\right.$$
$$\left. + \left(\frac{\nu_2}{28.4}\right)^{\beta_{\rm s}}\left(\frac{\nu_1}{353}\right)^{\beta_{\rm d}-2}\frac{B_{\nu_1}(T_{\rm d})}{B_{353}(T_{\rm d})}\right] \qquad T_{\rm d} = 19.6\,{\rm K}$$

This model does not include spectral decorrelation.

7 model parameters:

- synchrotron and dust amplitudes $A_{\rm s}$ and $A_{\rm d}$.
- two spectral indices $\beta_{\rm s}$ and $\beta_{\rm d}$.
- Two spatial spectral indices α_s and α_d
- dust/synchrotron polarization correlation parameter ρ .

Planck 2018 results: dust angular power spectra

Nested sky regions

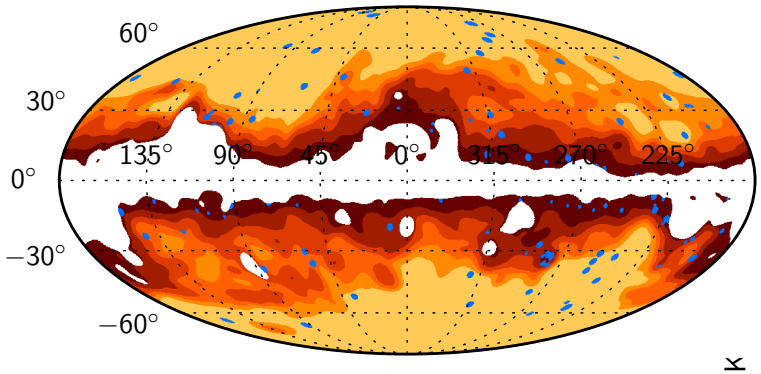

353 GHz angular power spectra

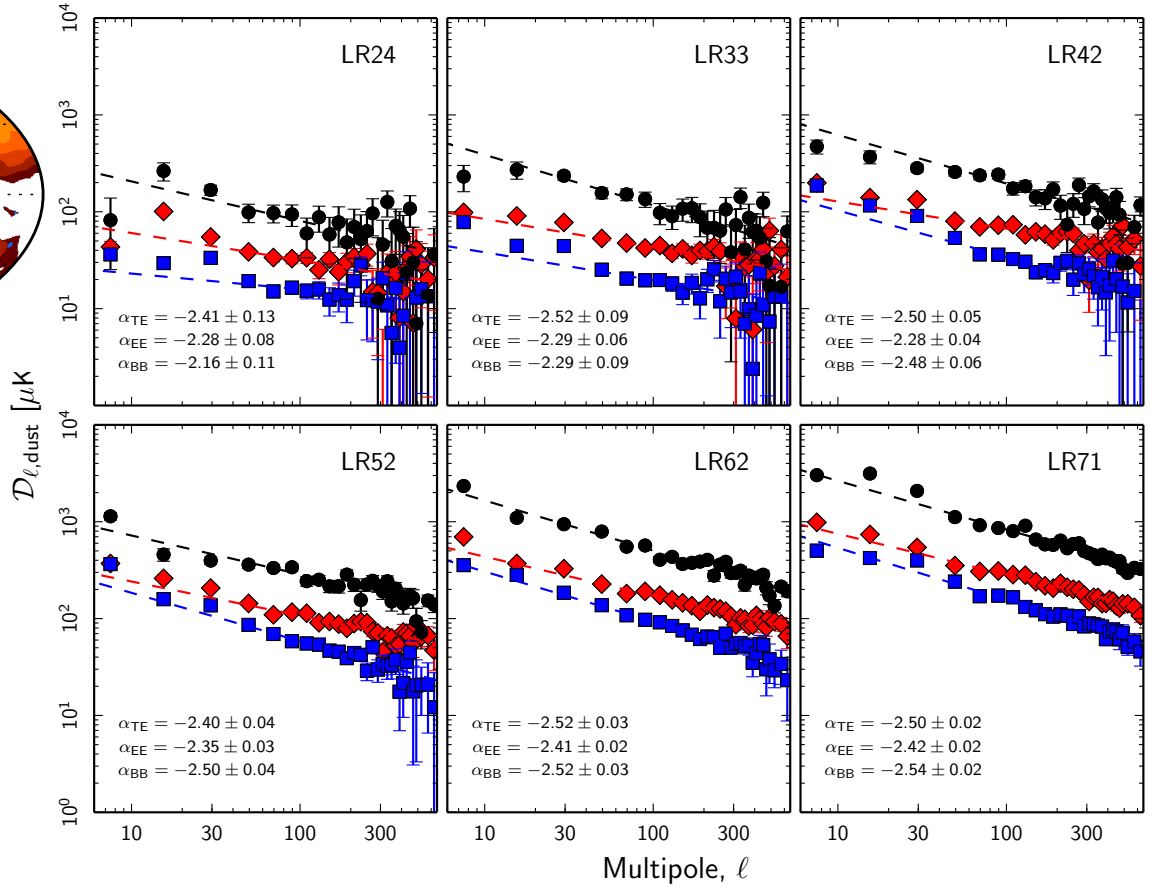

Planck HFI 353 GHz data allow to measure dust power spectrum over large sky portions, up to sub-degree scales

- The power-law exponents for ***EE*** and ***BB*** are slightly different.
- Spectra are not well fitted by a single power-law over the full multipole range.
- The ***E*/*B*** asymmetry and ***T*-*E*** correlation extend to low multipoles.

Dust TB and EB correlation

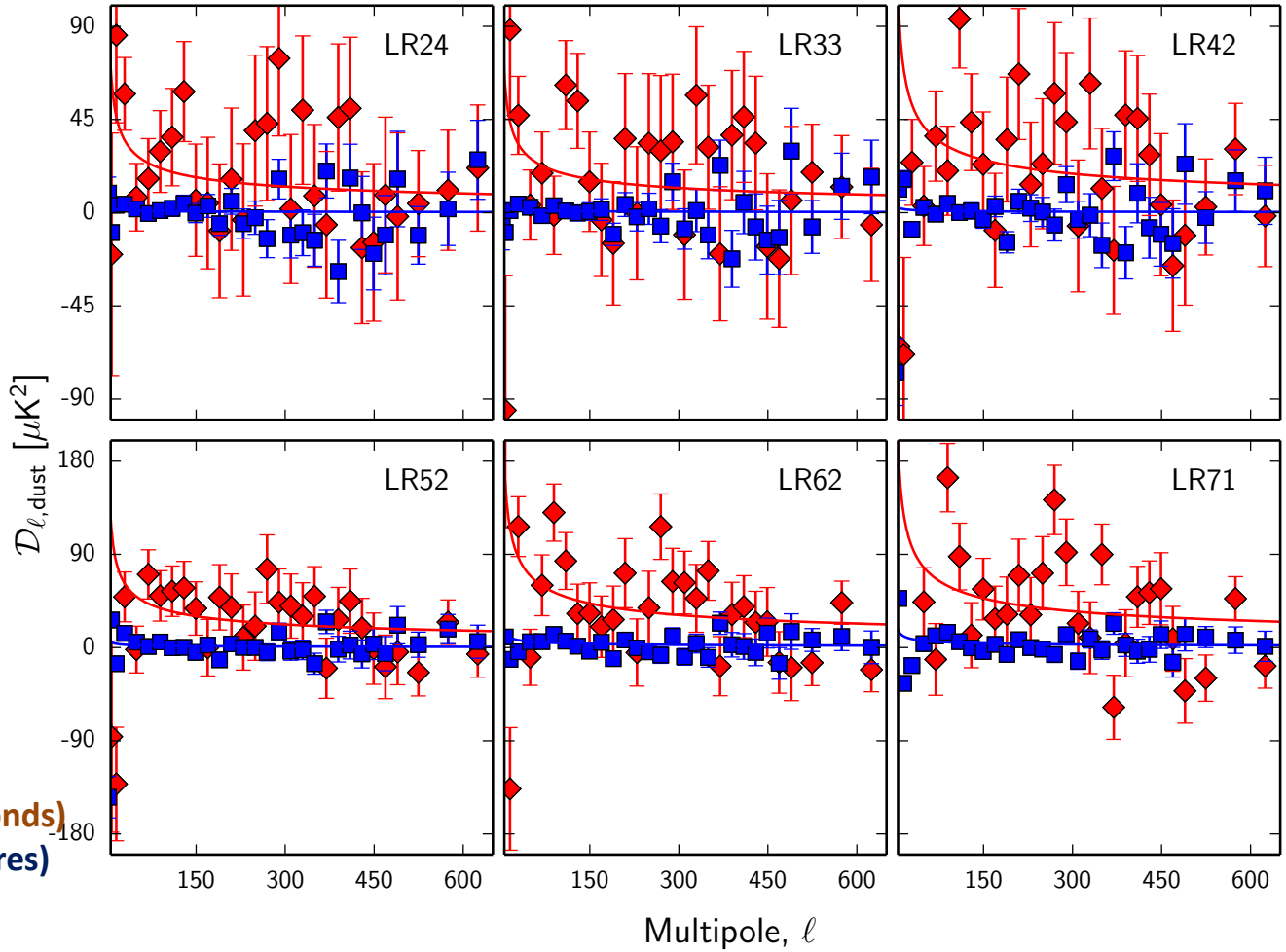

***TB* (red diamonds)**
***EB* (blue squares)**

Planck results XI 2018

- ***E-B*** correlation consistent with zero
- Evidence for positive ***T-B*** correlation. Non-zero dust ***T-B*** could have an impact on experiments calibrating the absolute polarization angle by minimizing this quantity
- Possible physical explanation related to filament magnetic field misalignment (***Clark et al. 2021***).

Dust *E-B* asymmetry

T-E correlation ratio

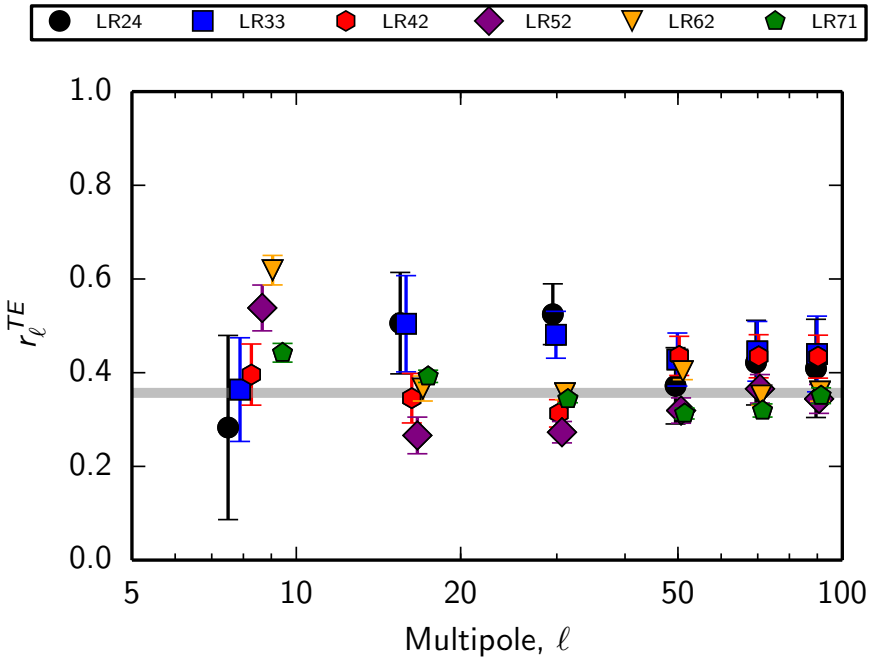

$$r_\ell^{TE} = \frac{C_\ell^{TE}}{\sqrt{C_\ell^{TT} \times C_\ell^{EE}}}$$

E-B asymmetry

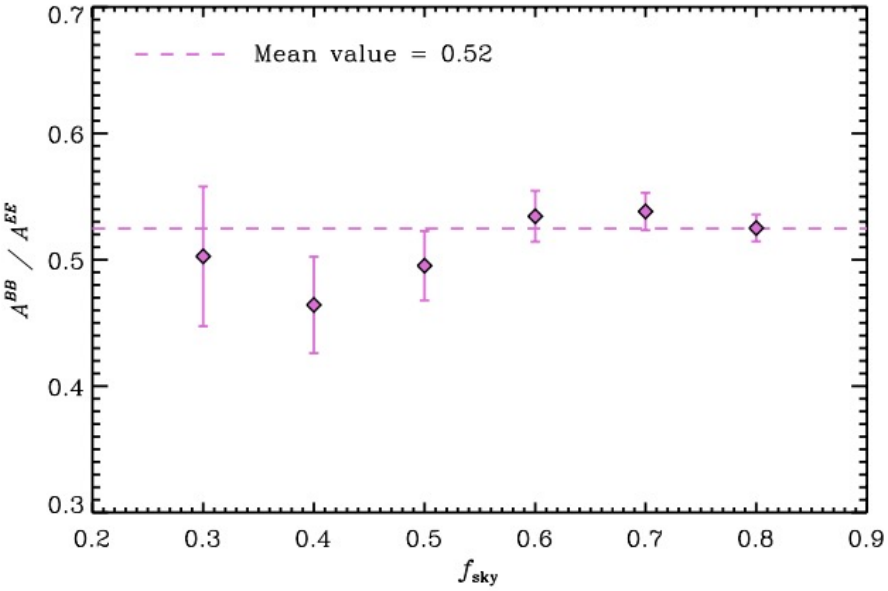

Polarized dust emission produces about half as much as *B*-mode power as *E*-mode power.

Planck results XI 2018
Planck intermediate results XXX 2015

E- and B-modes of interstellar filaments

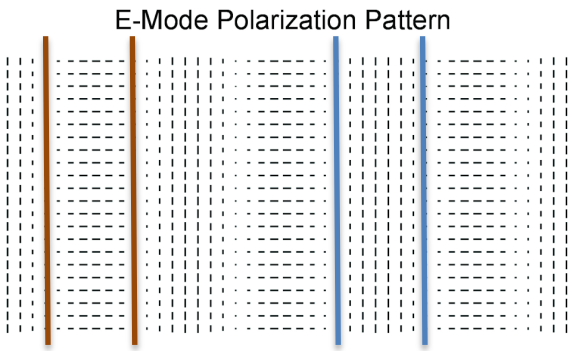

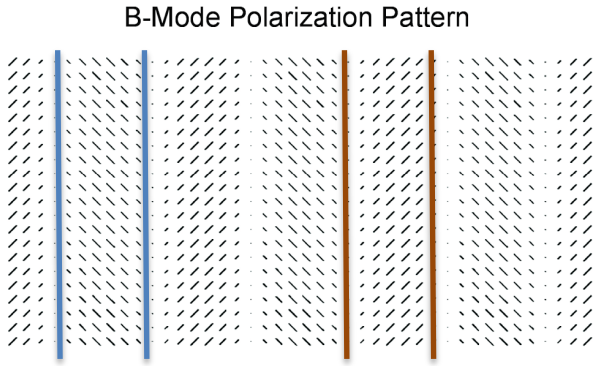

Zaldarriaga, PRD 64, 2001

Example filament (raw 353 GHz data)

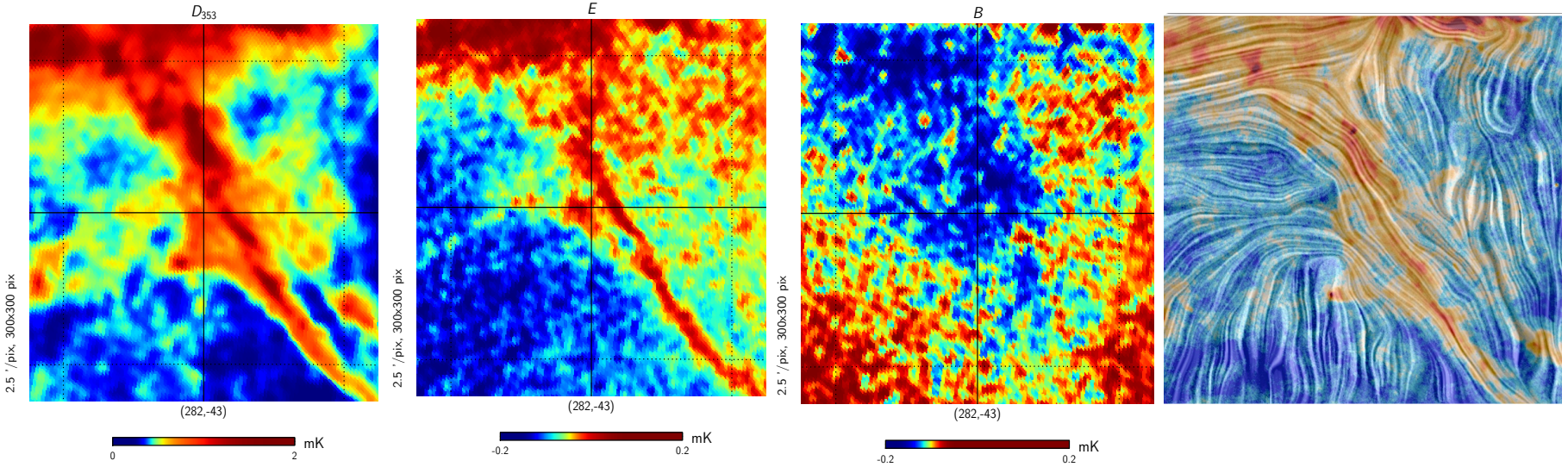

If a filament is preferentially aligned with the local direction of magnetic field, it produces more E-mode than B-mode.

Stacking of interstellar filaments

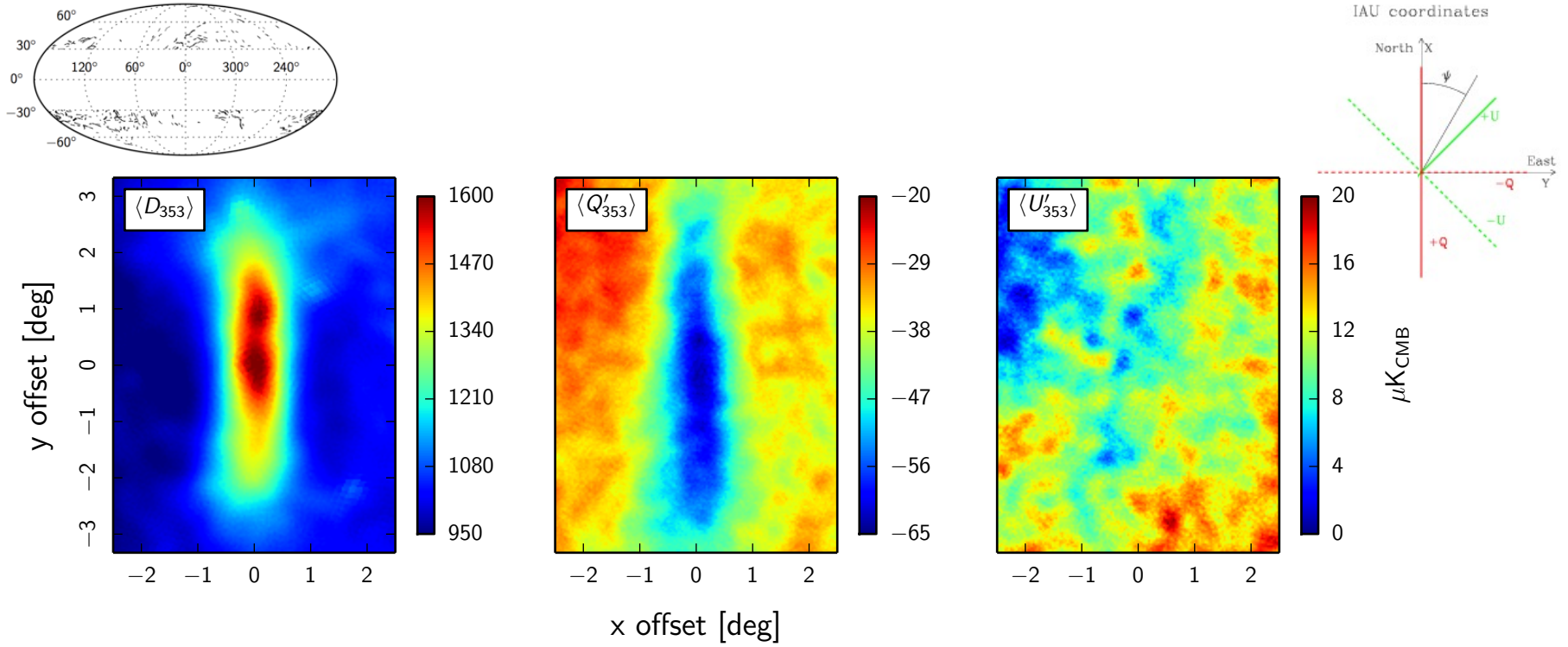

- Q' and U' are the Stokes Q and U maps computed with respect to the axis of the filament.
- The average filament appears as a negative feature with respect to the background in <Q'> image and is not seen in <U'> image.
- The 1 sigma uncertainty on the <Q'> and <U'> images is 1.3 uK_{CMB}.
- The homogeneous background in the <Q'> and <U'> images reflects the smoothness of B_{POS} over the patch size of 7x5 square degrees.

Planck XXXVIII 2015

Dust *B*-mode amplitude scaling with intensity

- ***BB*** power well fitted by $(I_{353})^2$
- BICEP region's Planck dust ***BB*** power is compatible with (but lower than) the fit on larger masks

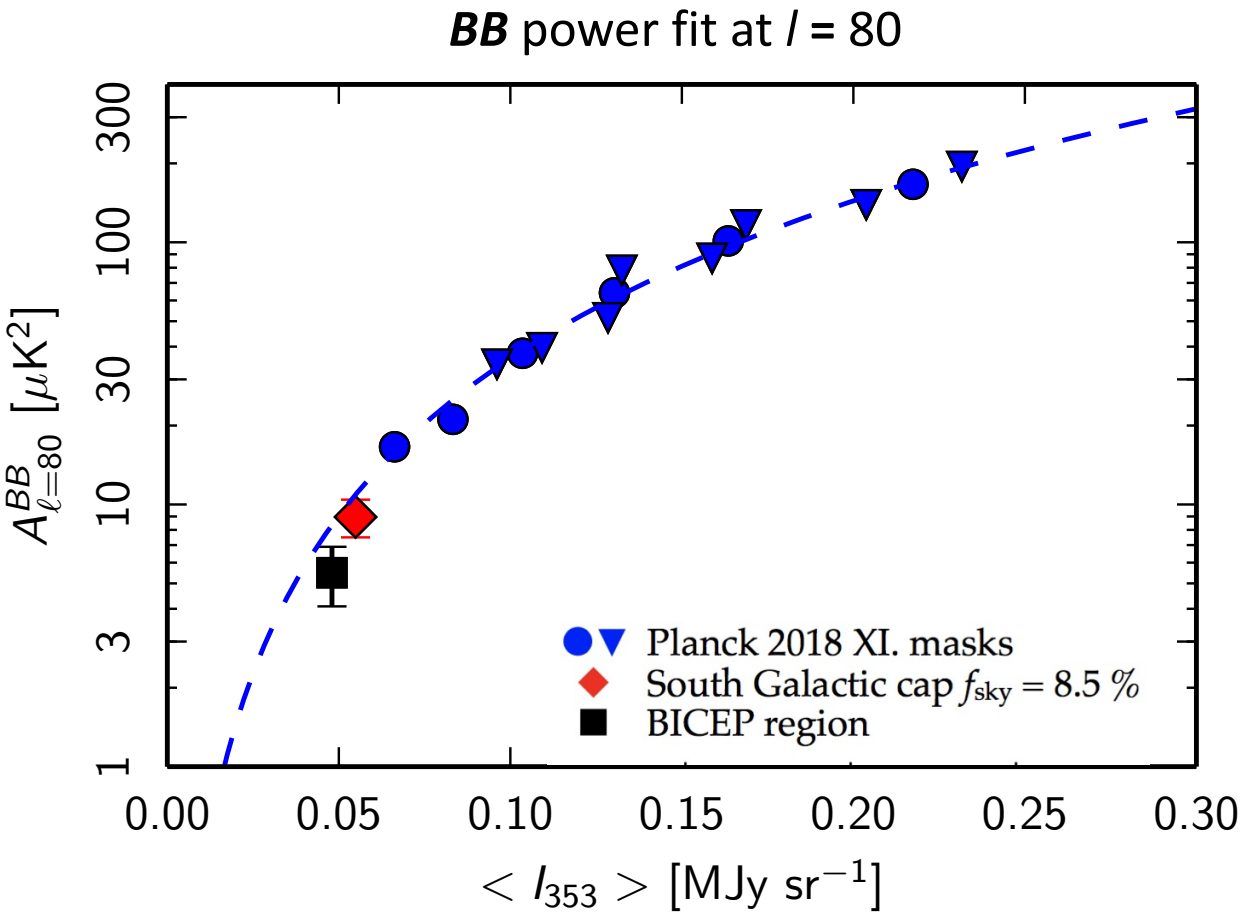

LR62 BB spectra

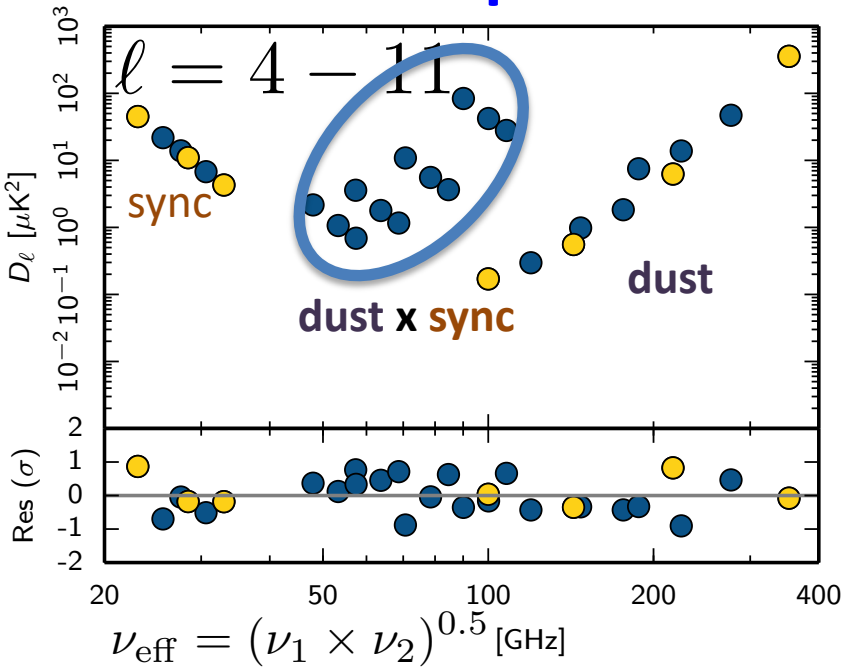

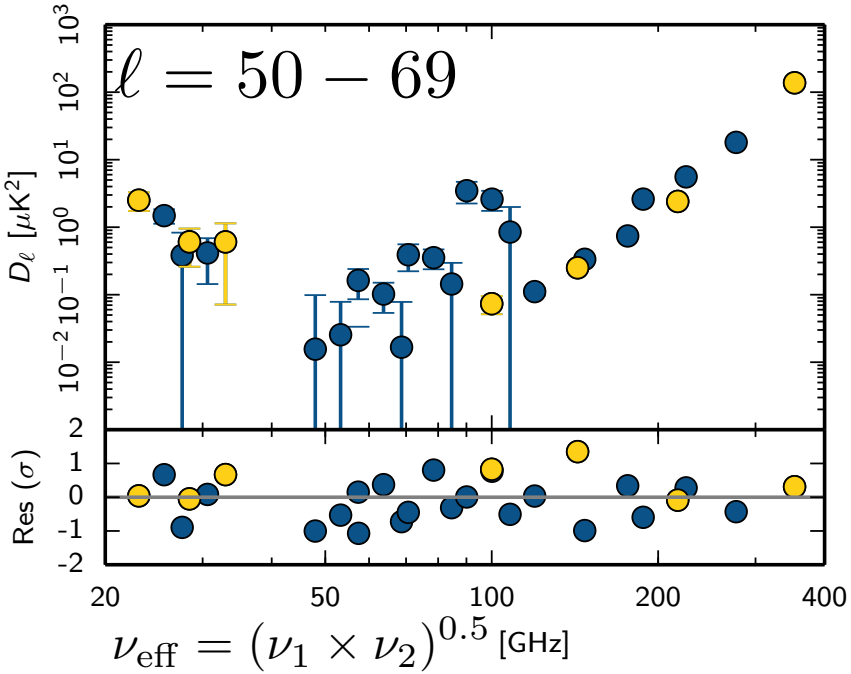

Dust-synchrotron correlation

- Dust-synchrotron correlation is strong at large angular scales and consistent with zero at small angular scales.
- The average of dust spectral index β_d ~ 1.53 +/- 0.02

Planck results XI 2018

Dust and synchrotron spectral parameters

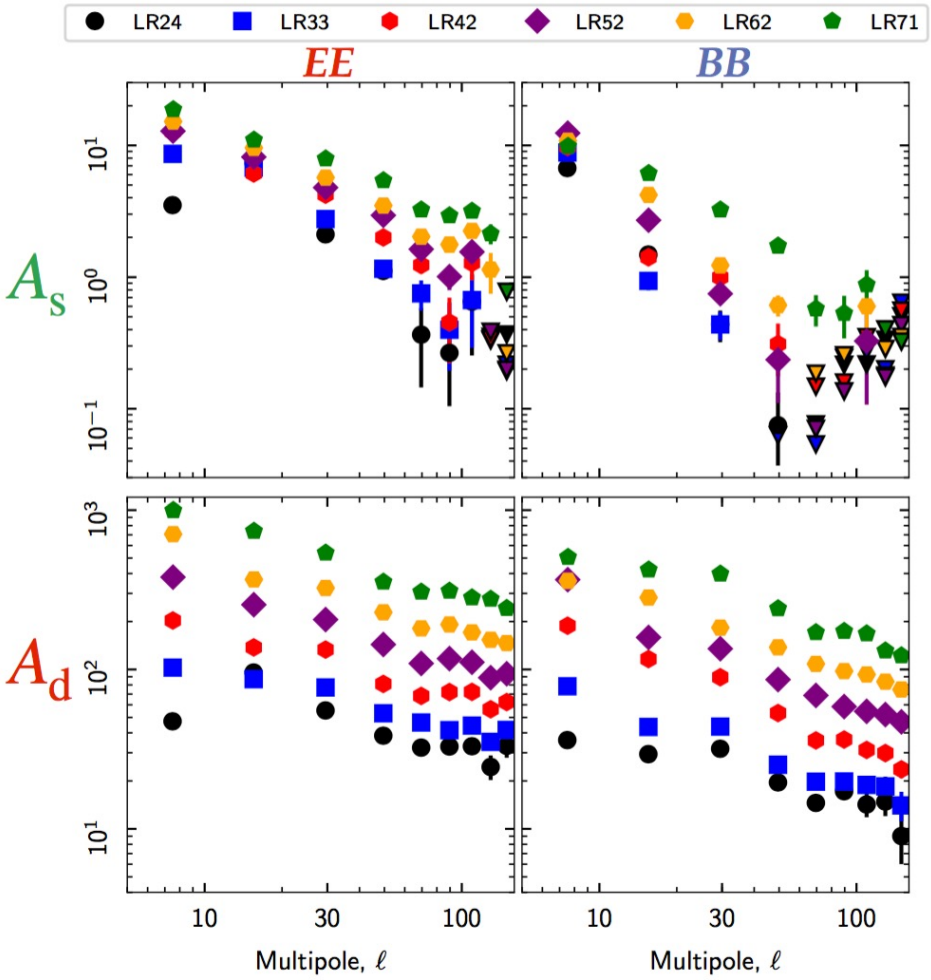

Inverted triangles = one sigma upper limit

BB A_s/A_d ratio is maximum at low multipoles and for the smallest sky region (LR24)

Dust and synchrotron spectral parameters

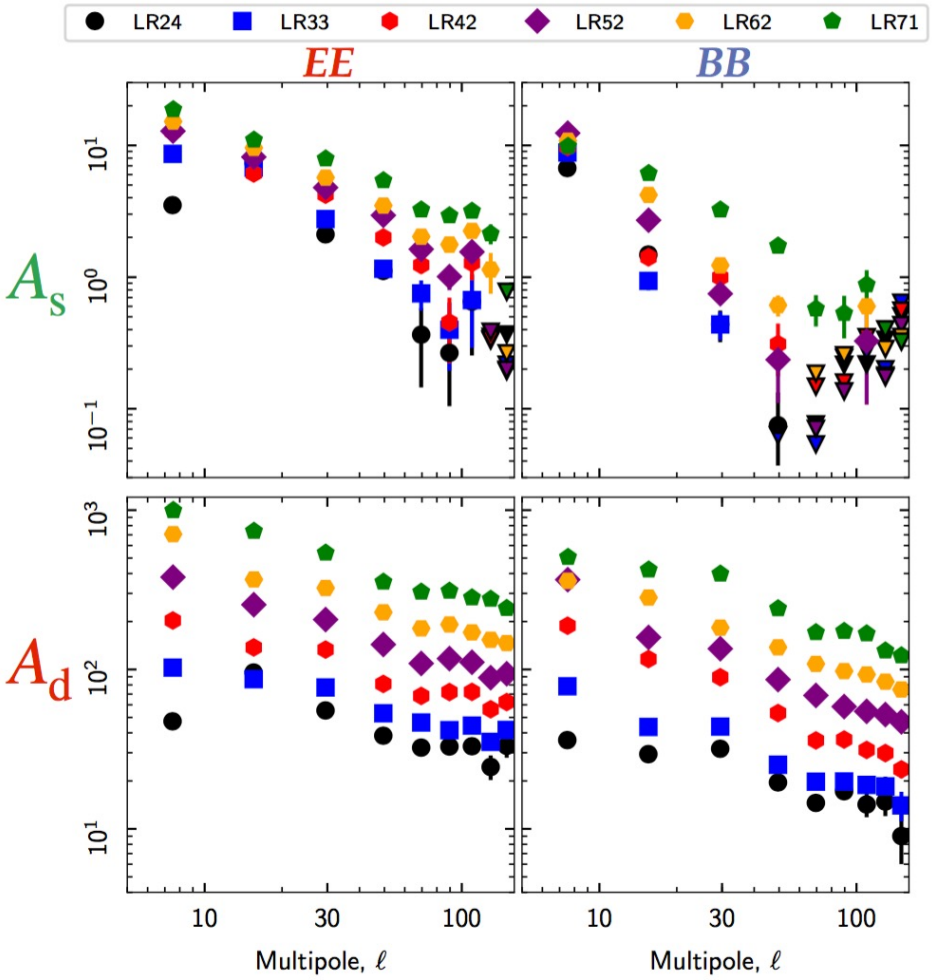

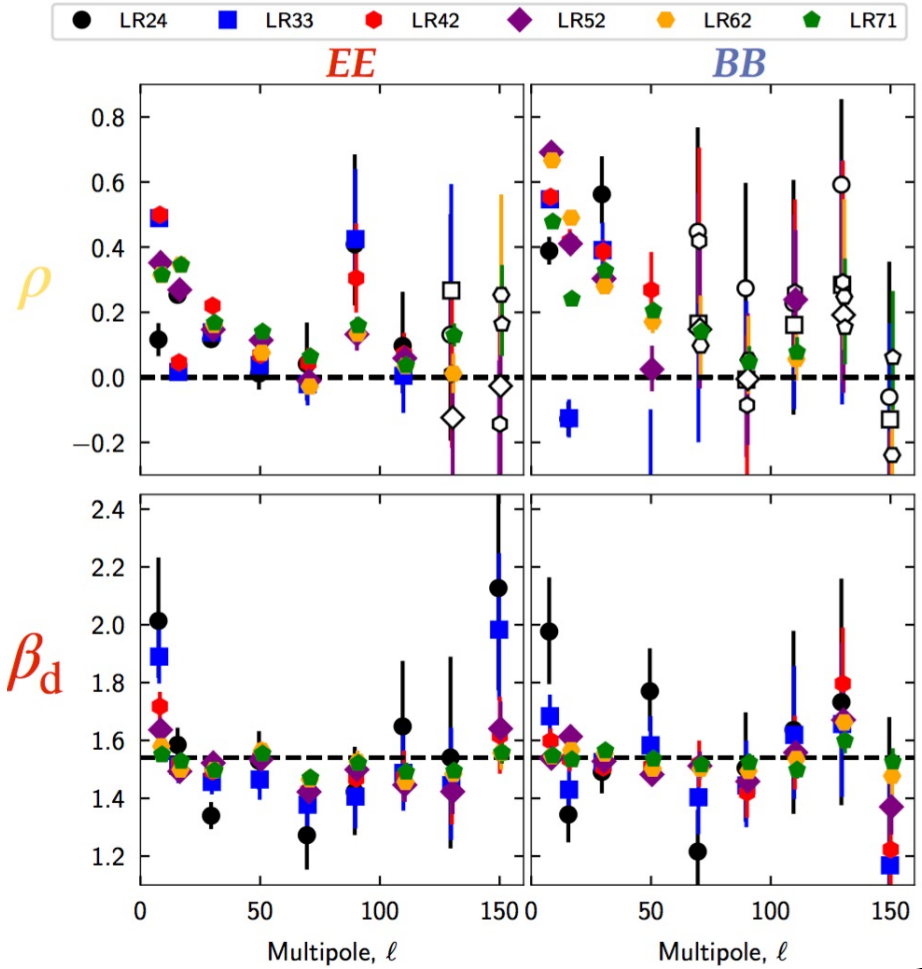

Inverted triangles = one sigma upper limit

BB A_s/A_d ratio is maximum at low multipoles and for the smallest sky region (LR24)

- Significant dust-synchrotron correlation at $l \lesssim 50$
- No evidence for dust spectral index l dependence

Dust spectral energy distribution

Dust SED in polarization

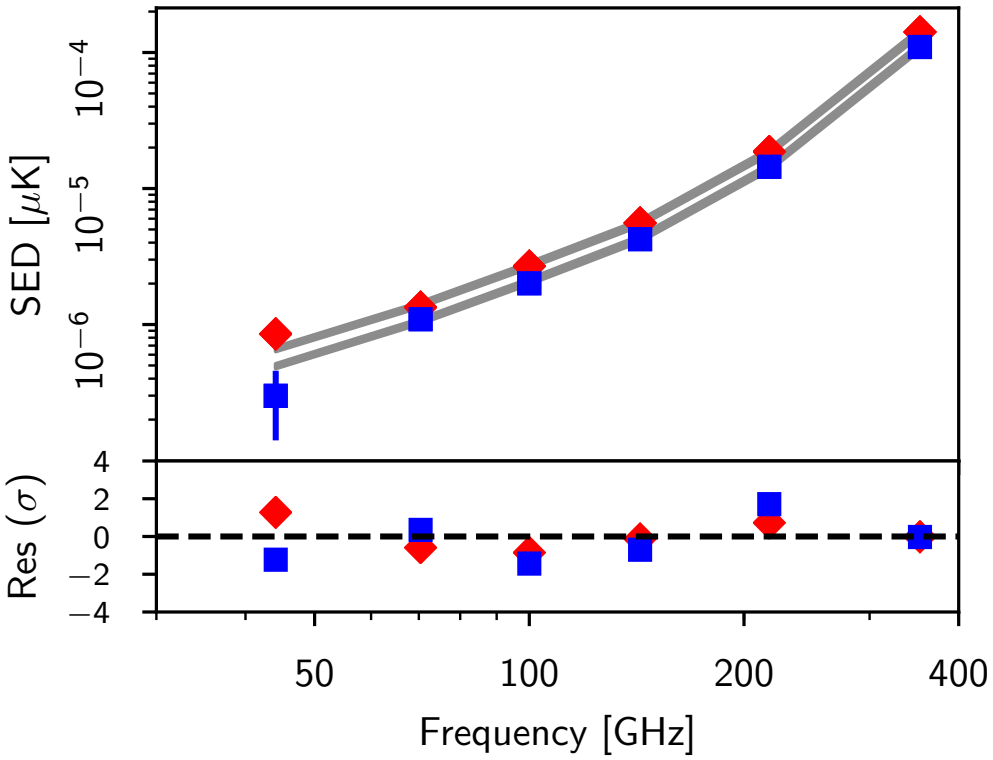

- In polarization, the dust SED from SMICA component separation method fits well by a single temperature modified black-body emission law from 353 GHz to 44 GHz.

Polarization vs total intensity

- The difference between spectral indices for polarization and total intensity is small (0.05 ± 0.03) and not of high statistical significance
- Planck data analysis suggests that the emission from a single grain type dominates the long-wavelength emission in both polarization and total intensity.

Dust decorrelation

Stacking of small number of polarized emission layers, with plane-of-sky spatial correlations

$$\boldsymbol{B} = \boldsymbol{B}_0 + \boldsymbol{B}_t$$

Turbulent field

Uniform field

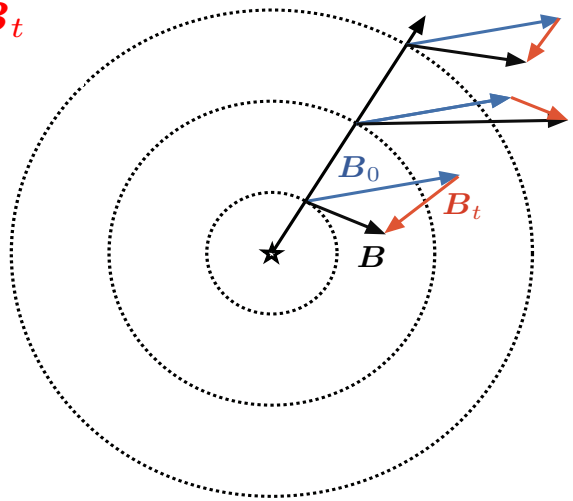

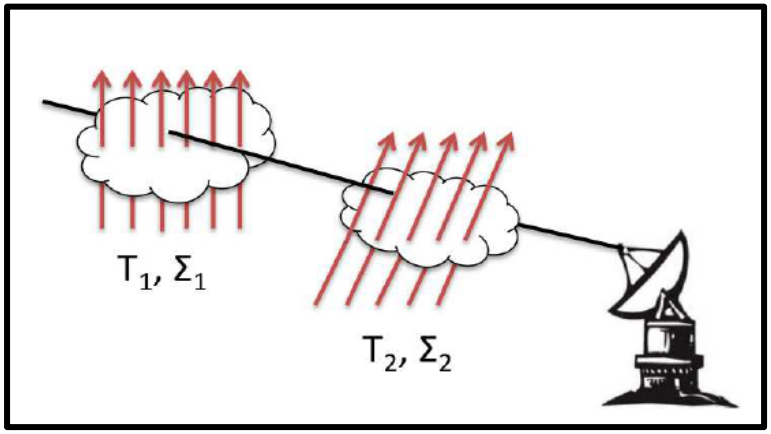

Tassis and Pavlidou, 2015, MNRAS

Toy example

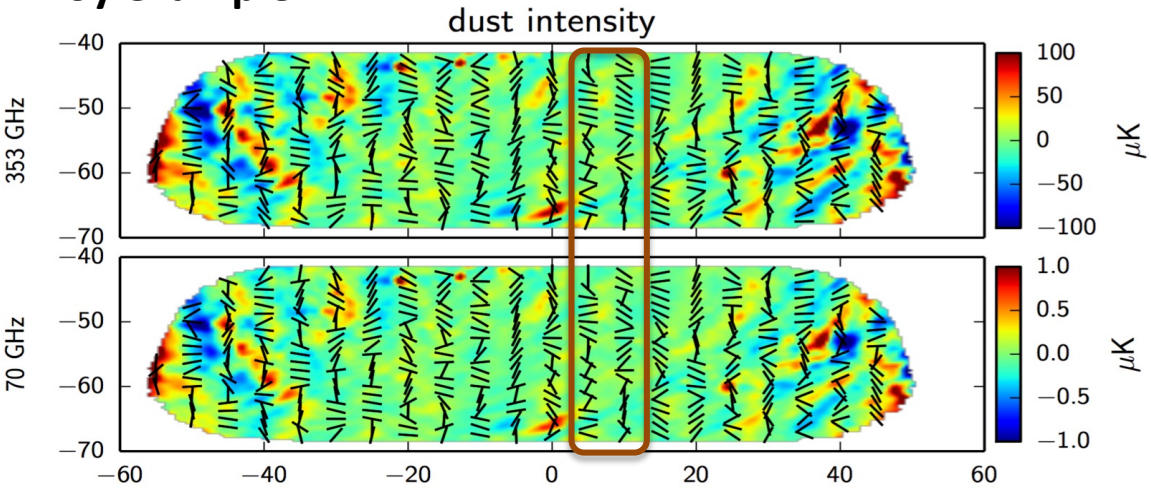

Correlation ratio of dust *B*-modes between two different frequencies is measured as

$$R_\ell^{BB} = \frac{\mathcal{D}_\ell^{BB}(\nu_1 \times \nu_2)}{\sqrt{\mathcal{D}_\ell^{BB}(\nu_1 \times \nu_1) \times \mathcal{D}_\ell^{BB}(\nu_2 \times \nu_2)}}$$

Vansyngel et al. 2017, A&A

Ghosh et al. 2017, A&A

Spatial decorrelation of dust B-modes

Correlation ratio between 217 and 353 GHz maps

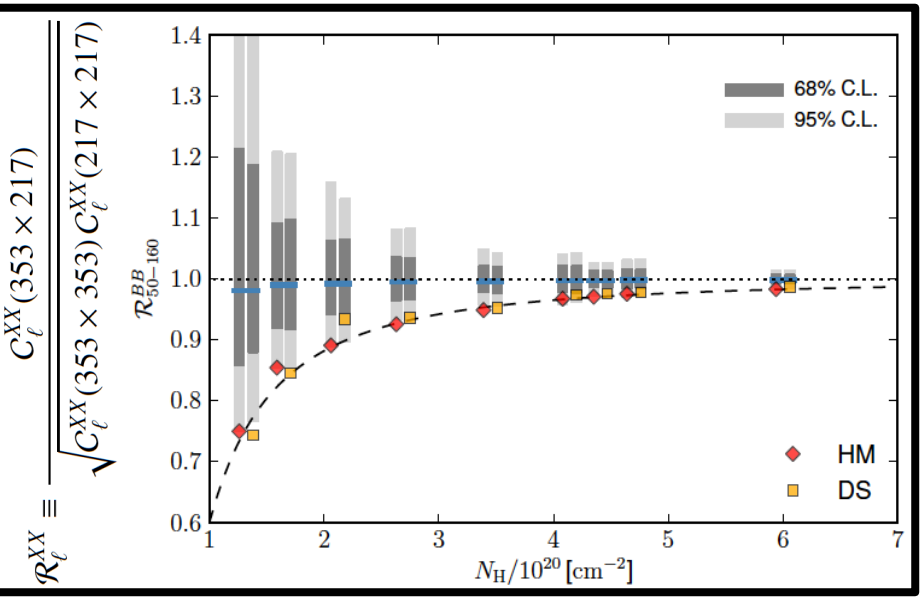

As a function of angular scale

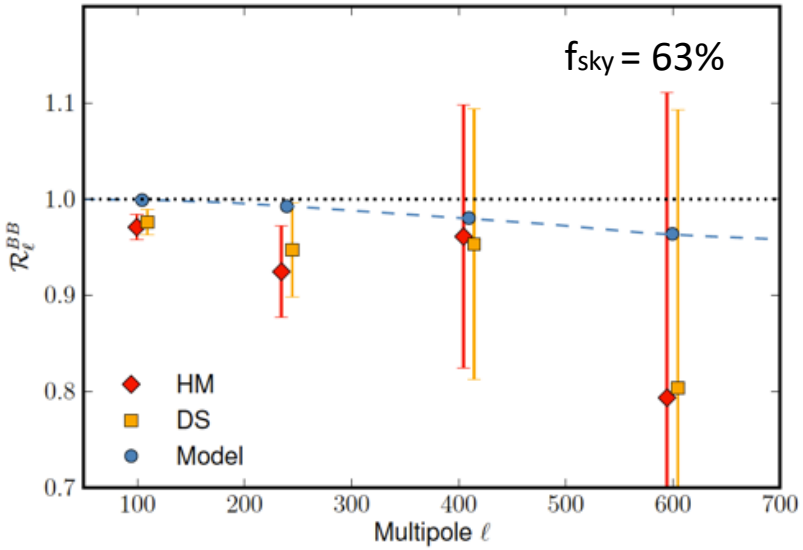

- Correlation ratio (*BB*) measured for several sky regions (f_{sky}=0.2 to 0.8) with cross-spectra using different data subsets.
- Confidence estimated with Gaussian sky simulations.
- The effect is (marginally) detected in all regions.
- Indication that the dust decorrelation increases towards low column density regions.

Planck Intermediate results. L 2016

Vansyngel decorrelation model

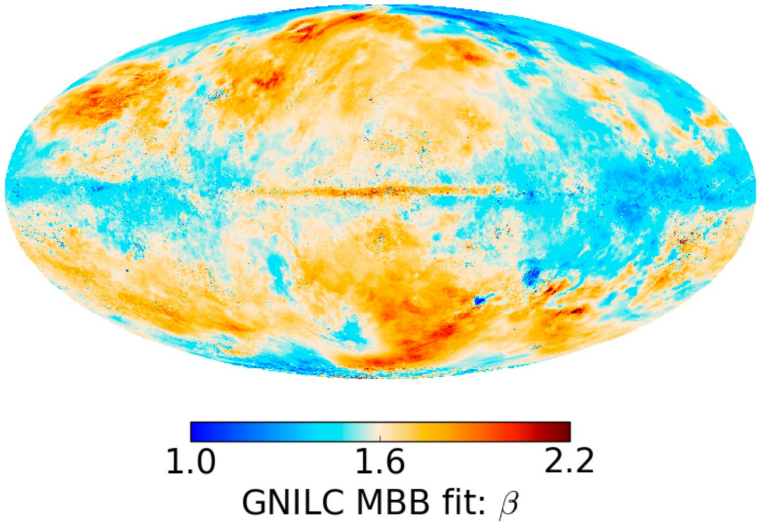

SED variations

Amplitude of cross-spectra between HFI frequencies ν_1 and ν_2 :

$$\mathcal{D}_\ell(\nu_1 \times \nu_2) = A_{\rm d} \left(\frac{\nu_1 \nu_2}{353^2}\right)^{\beta_{\rm d}-2} \frac{B_{\nu_1}(T_{\rm d})}{B_{353}(T_{\rm d})} \frac{B_{\nu_2}(T_{\rm d})}{B_{353}(T_{\rm d})} R_\ell(\delta_{\rm d}, \nu_1, \nu_2)$$

where

$$T_{\rm d} = 19.6\,{\rm K}$$

$$R_\ell(\delta_{\rm d}, \nu_1, \nu_2) = \exp\left[-\delta_{\rm d}\, \ln\left(\frac{\nu_1}{\nu_2}\right)^2\right]$$

One extra parameter $\delta_{\rm d}$

Assumes a frequency dependence model of spectral decorrelation based on ***Vansyngel et al. 2017***.

Dust frequency correlation

Frequency decorrelation due to effective SED spatial variations has to appear at some level

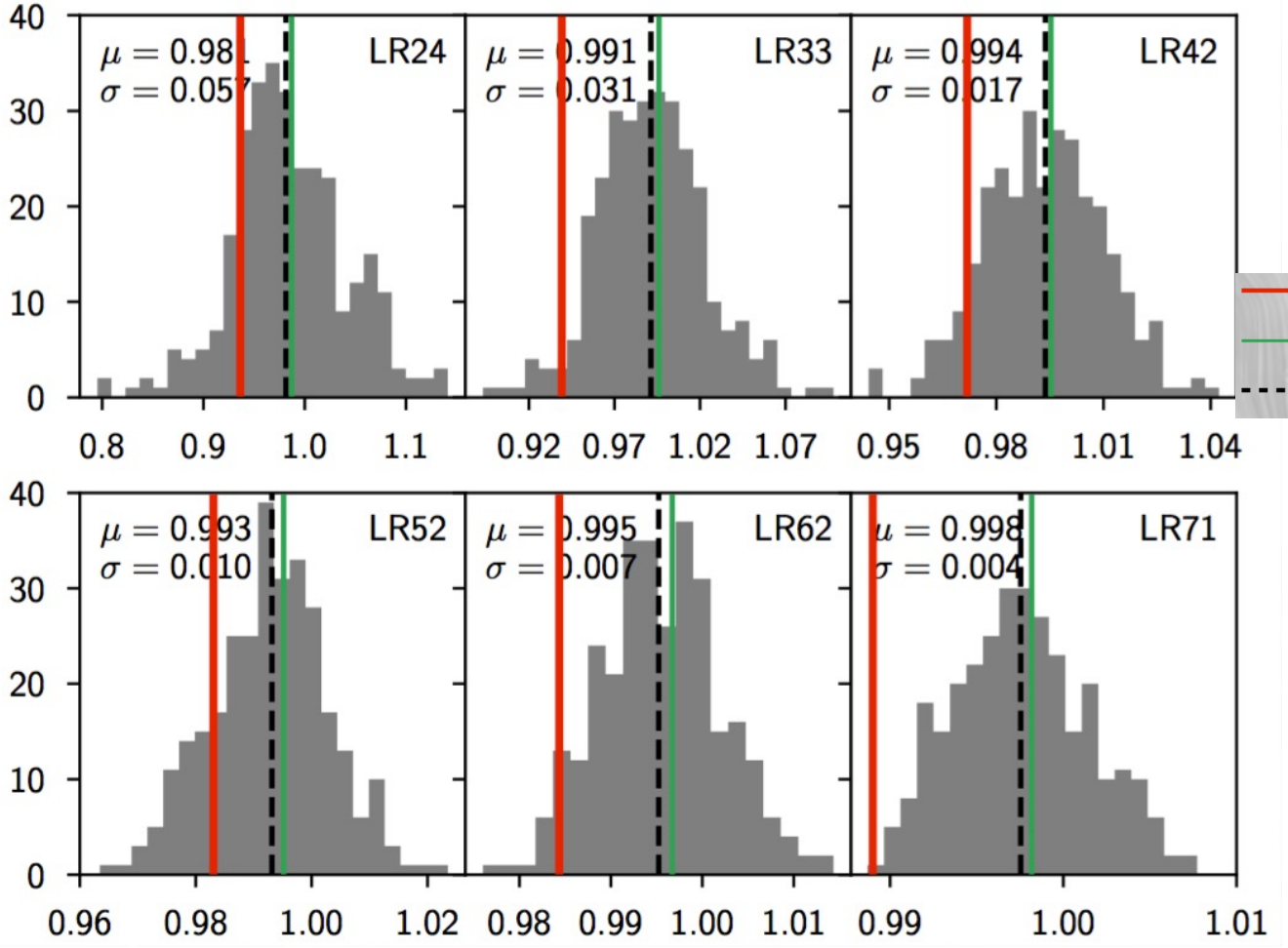

- results of HFI-only (100 – 353 GHz) multi-frequency fit over the multipole range 50 – 160.
- The mean of spectral correlation ratio is consistent with one within 1 sigma error-bars.

BICEP results in the presence of dust decorrelation

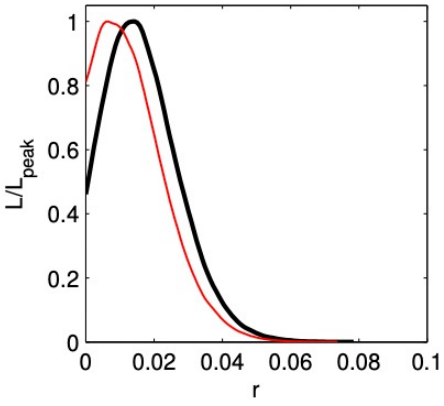

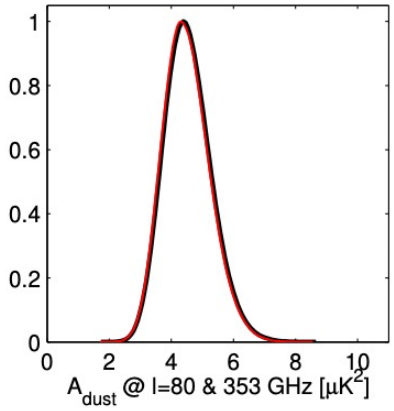

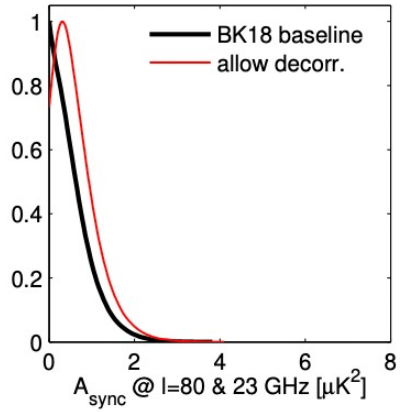

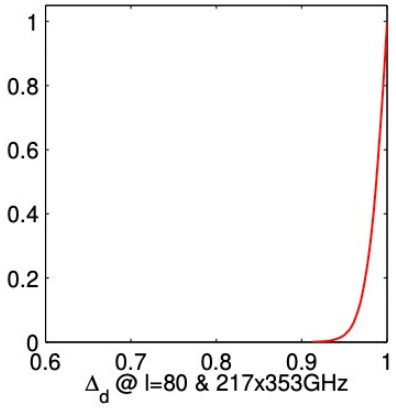

r < 0.036 (95% C.L)

BK18, PRL 2021

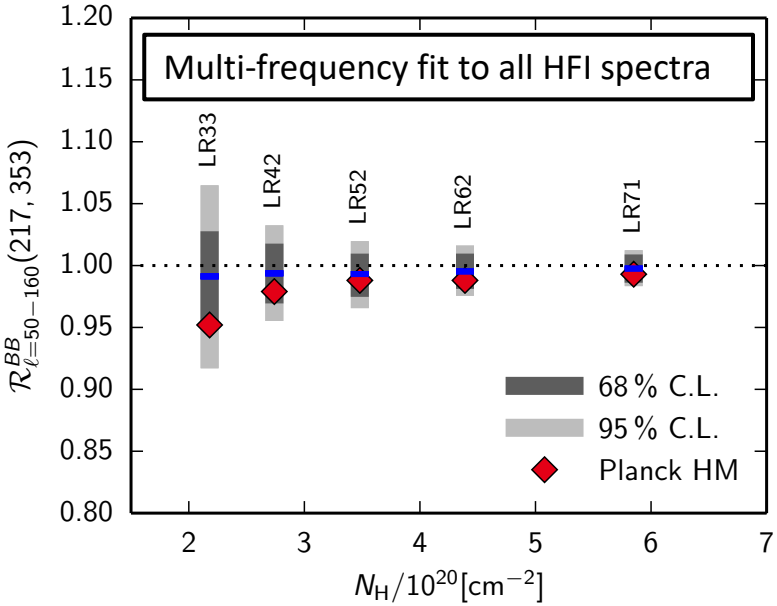

Implementation of multi-layer galaxy model

a. Divide the total column density into a set of layers.

b. Assign to each layer a different map of polarisation fraction and angle.

c. Assign to each layer a different map of emission law parameters.

a. Renormalise to match Planck dust polarization observations.

Layers of galactic emission

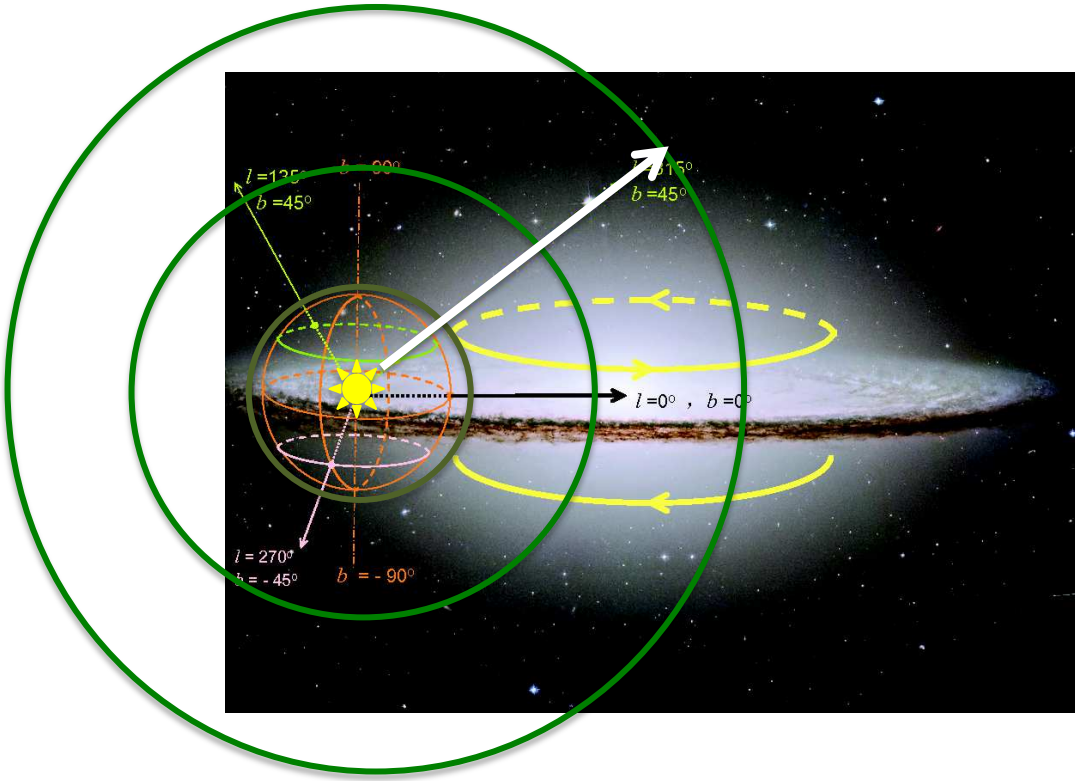

Line-of-sight integration

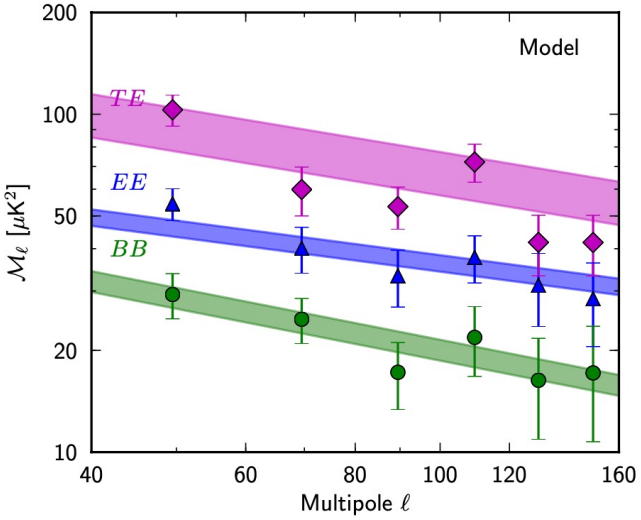

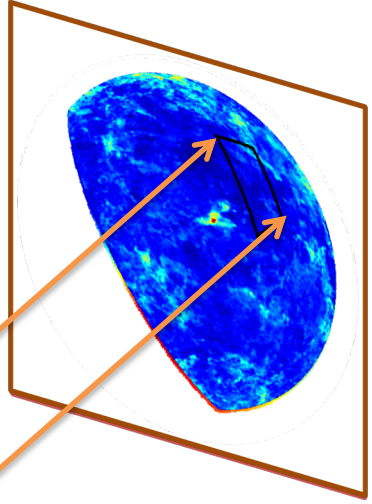

Dust in warm diffuse phase

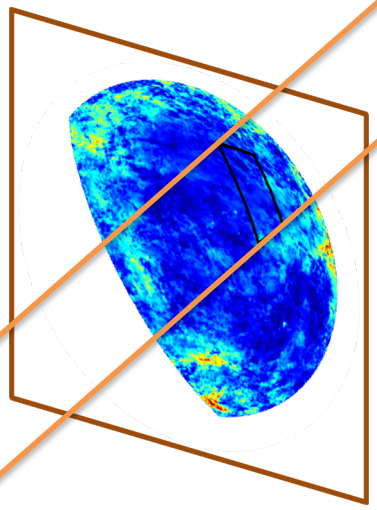

Dust in thermally unstable phase

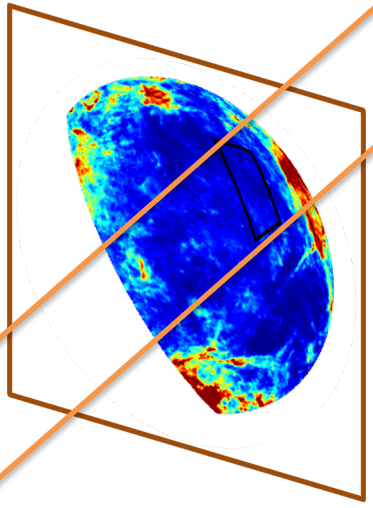

Dust in cold dense phase

Ghosh et al. 2017
Vansyngel et al. 2017
Adak et al. 2021

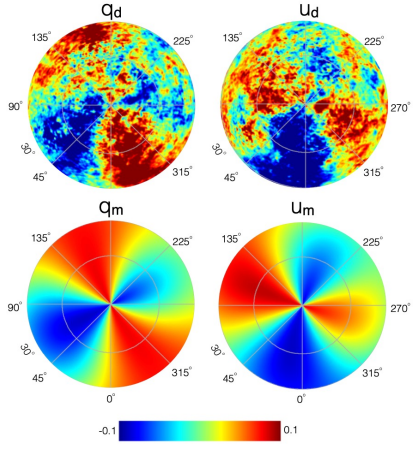

CMB-Bharat – '*r*' recovery

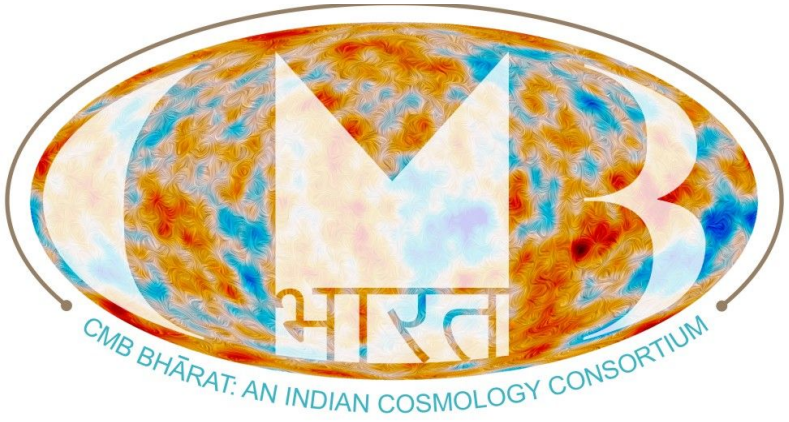

Table 1. ECHO instrument specification as proposed in the CMB-Bhārat proposal.

Frequency (GHz)	Beam FWHM (arcmin)	Q & U noise r.m.s (μK.arcmin)
28	39.9	16.5
35	31.9	13.3
45	24.8	11.9
65	17.1	8.9
75	14.91	5.1
95	11.7	4.6
115	9.72	3.1
130	8.59	3.1
145	7.70	2.4
165	6.77	2.5
190	5.88	2.8
220	5.08	3.3
275	4.06	6.3
340	3.28	11.4
390	2.86	21.9
450	2.48	43.4
520	2.14	102.0
600	1.86	288.0
700	1.59	1122.0
850	1.31	9550.0

Table 3. Set of simulations used in the analysis. The tick and cross symbols indicate which components are added and excluded respectively for different sets. The dust and synchrotron models used are identified using nomenclatures listed in Table 2.

Sim.ID	Pipeline		Dust	Synchrotron	AME	point-sources	delensing	Decorrelation
	Commander	NILC						
SET1a	✓	✓	GNILC – dust	GALPROP	✗	✗	✗	✗
SET1b	✓	✓	GNILC – dust	GALPROP	✓	✗	✗	✗
SET1c	✓	✓	GNILC – dust	GALPROP	✓	✓	✗	✗
SET1d	✓	✓	GNILC – dust	GALPROP	✗	✗	✓(84 %)	✗
SET1e	✓	✓	GNILC – dust	Power – law	✓	✓	✗	✗
SET1f	✓	✓	GNILC – dust	Curved–power–law	✓	✓	✗	✗
SET2a	✓	✓	Gines – dust	GALPROP	✓	✓	✗	✓
SET2b	✓	✓	Gines – dust	Power – law	✓	✓	✗	✓
SET2c	✓	✓	Gines – dust	Curved–power–law	✓	✓	✗	✓
SET3a	✓	✗	TD – dust	GALPROP	✓	✓	✗	✗
SET3b	✓	✗	TD – dust	GALPROP	✓	✓	✗	✓

- To detect r ~ 10^{-3} at 3σ significance
- 20 frequency bands between 28 and 850 GHz
- CMB polarization sensitivity: 1-2 uK.arcmin

Adak et al. 2022

Component separation results

Input r = 0

Commander results

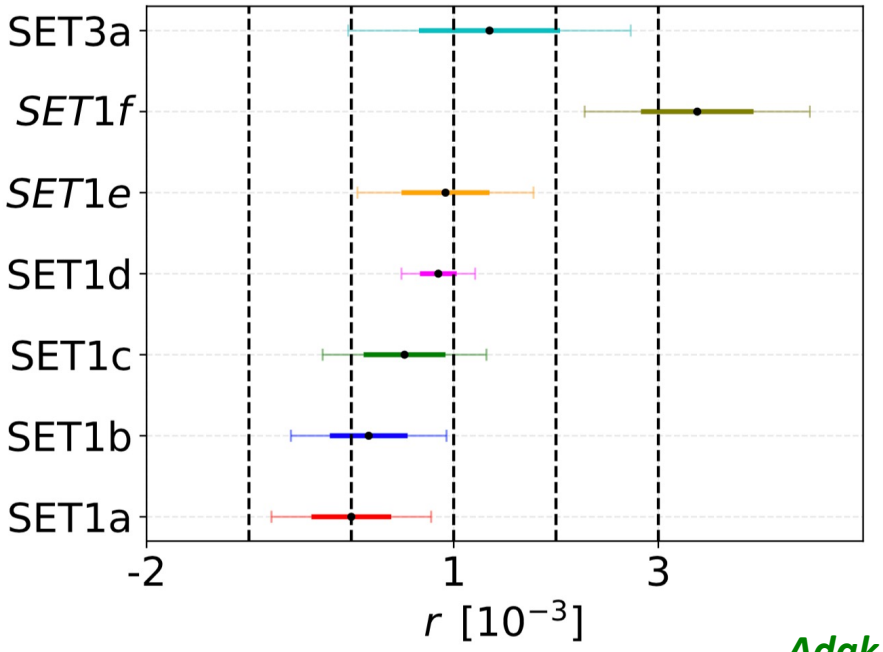

NILC results

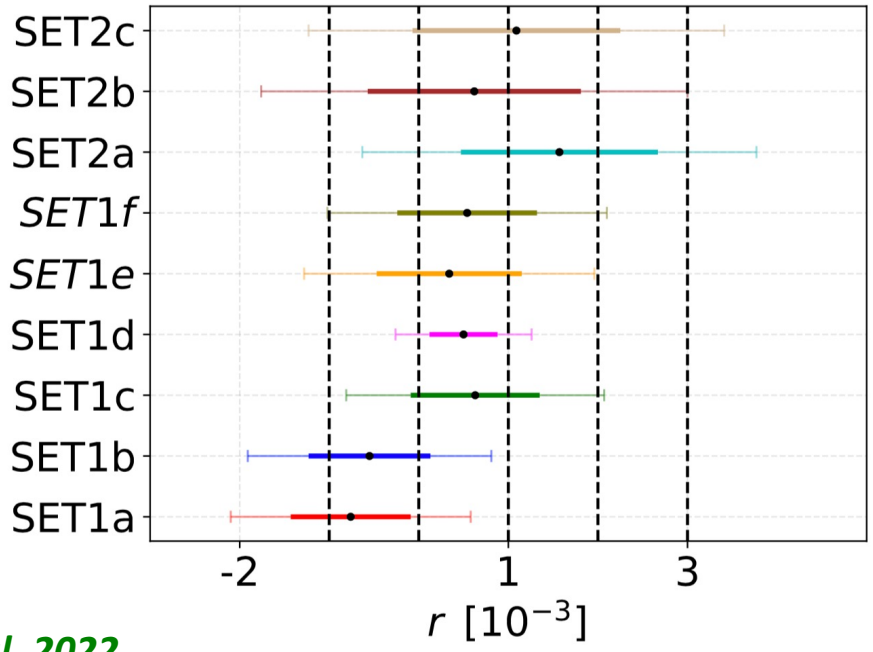

Adak et al. 2022

- ✓ COMMANDER returns biased *r* values for curved power-law synchrotron model.
- ✓ COMMANDER returns biased *r* values in the presence of dust decorrelation.
- ✓ NILC handles well different emission law models of synchrotron, e.g. curved power law.
- ✓ NILC returns larger errorbar on *r* in the presence of dust decorrelation.

Summary

- Analysis of Planck, WMAP and ground-based CMB observations (BICEP/Keck, SPT, ACT, QUIJOTE, SPASS, CBASS) allowed a deeper understanding of foreground properties, complexities and contamination to CMB polarization.

- Foreground properties are mostly statistical and efforts are going on to include in the sky models like PSM and PysM with the expected level of complexity.

- This have triggered efforts in developing new component separation techniques.

- Foreground study is important to build robustness test for any future claim on new CMB discoveries (statistical isotropy, non-Gaussianity etc..).

Synchrotron spectral energy distribution

WMAP 23GHz x Planck 30GHz *Martire et al. 2022*

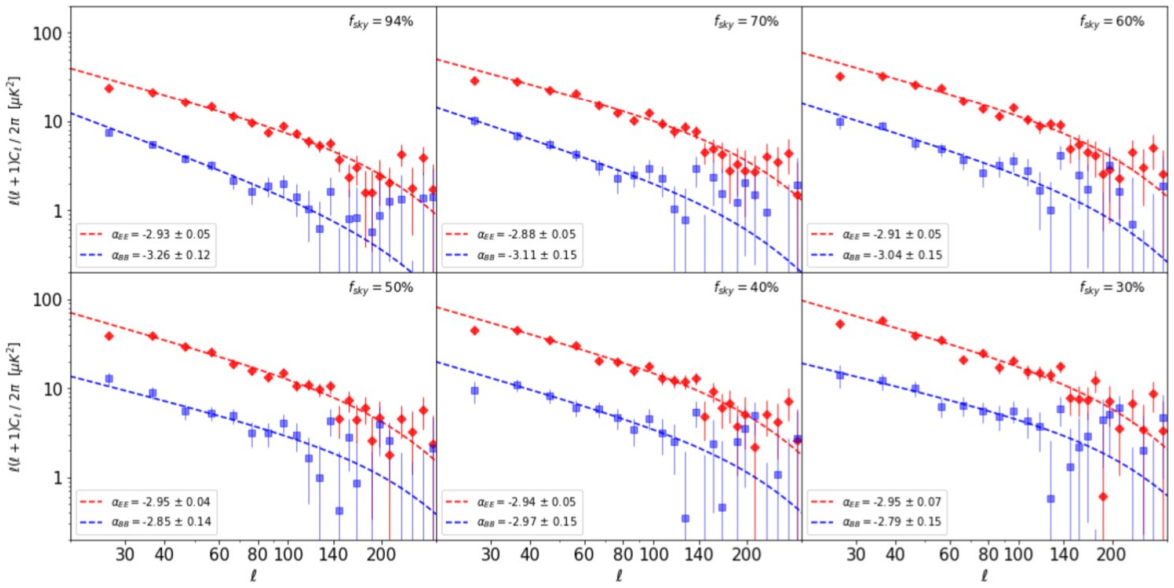

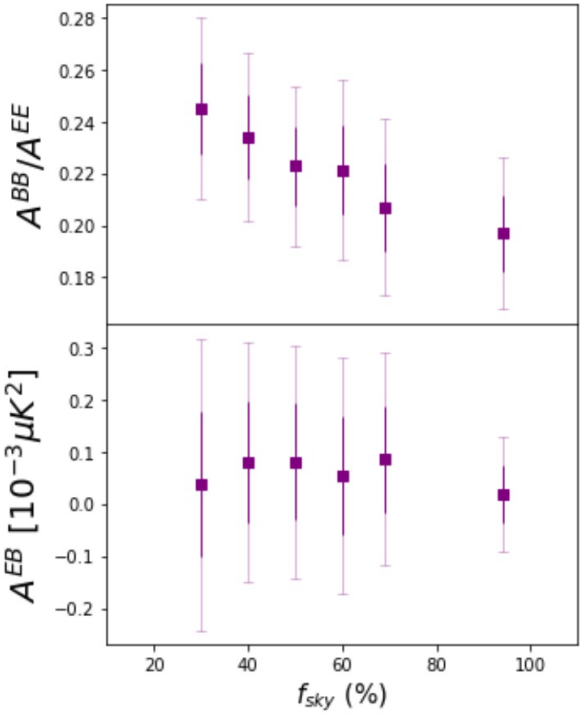

- ***E-B*** correlation consistent with zero
- **BB/EE** ratio <= 0.25 (large E-B asymmetry)
- Synchrotron power spectrum show steeper slope with respect to thermal dust (constraint up to ell = 200 over larger sky portions)

Synchrotron SED combining SPASS and Planck/WMAP

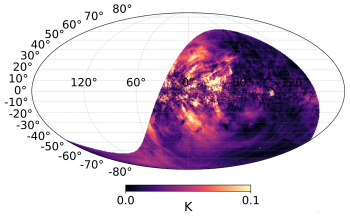

$$D_\ell(\nu_1 \times \nu_2) = A_s \left(\frac{\nu_1}{\nu_0}\right)^{\beta_s + s_{run}\log(\nu_1/\nu_0)} \left(\frac{\nu_2}{\nu_0}\right)^{\beta_s + s_{run}\log(\nu_2/\nu_0)}$$

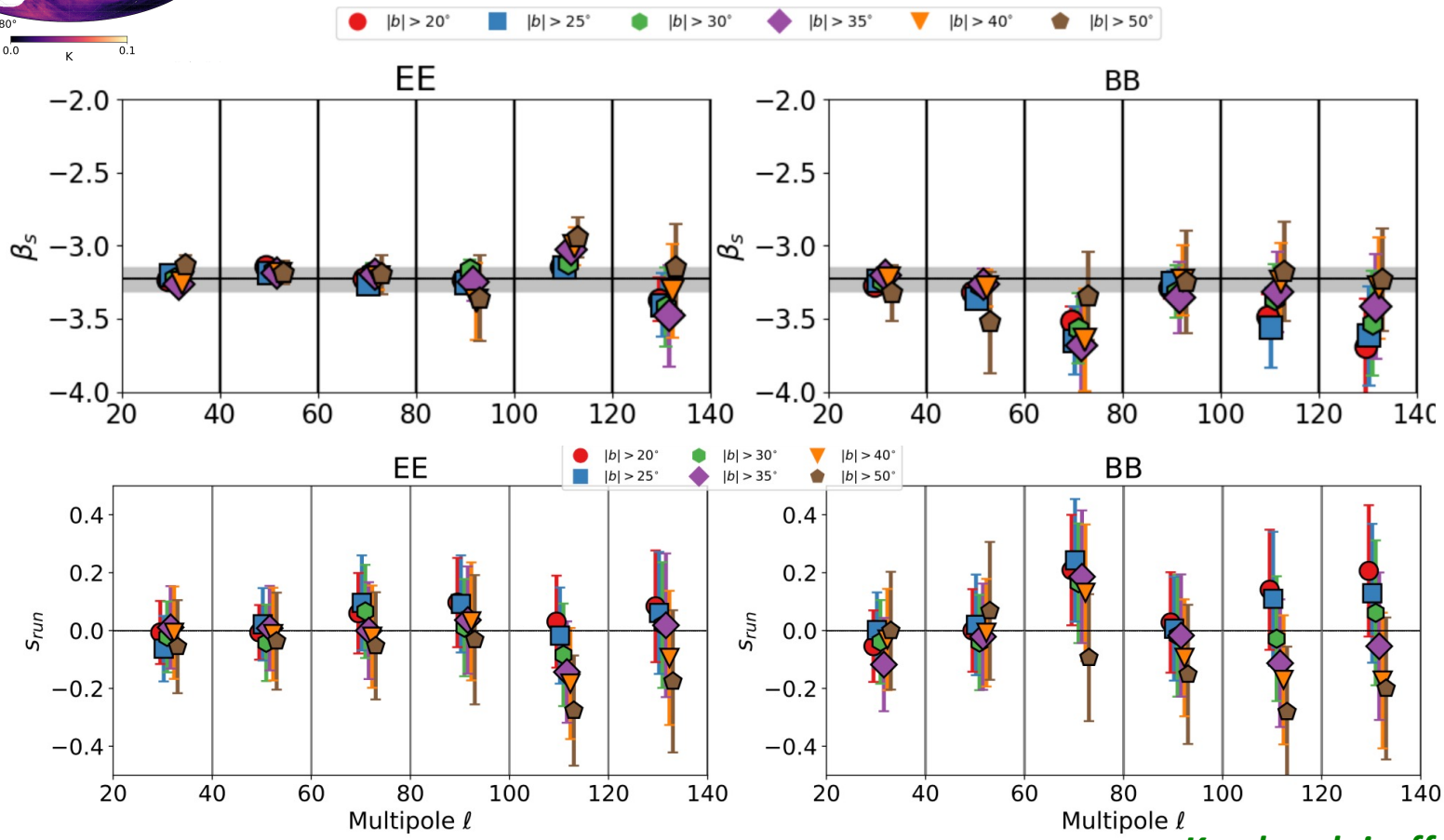

Krachmalnicoff et al. 2018

- Strong degeneracy between β_s and s_{run}
- **Gaussian prior on spectral index** from WMAP and Planck: $\beta_s = -3.13 \pm 0.13$
- s_{run} **compatible with zero**, with 1σ errors between 0.07 and 0.14